NASA

Technical Memorandum 83898

Spectra of Cosmic X-Ray Sources

Stephen S. Holt and
Richard McCray

FEBRUARY 1982

National Aeronautics and
Space Administration

Goddard Space Flight Center
Greenbelt, Maryland 20771

SPECTRA OF COSMIC X-RAY SOURCES

Stephen S. Holt

Laboratory for High Energy Astrophysics

NASA-Goddard Space Flight Center

Greenbelt, MD 20771

Richard McCray

Joint Institute for Laboratory Astrophysics

University of Colorado and National Bureau of Standards

Boulder, CO 80309

To appear in Annual Reviews of Astronomy and Astrophysics, Vol. 20, 1982.

I. INTRODUCTION

A. Overview

X-ray measurements provide the most direct probes of astrophysical environments with temperatures exceeding 10^6 K. Since the initial discovery of extra-solar X-rays in 1962 (Giacconi et al. 1962) X-ray astronomy has evolved from a novelty to a major branch of astronomical research, reaching, with the launch of the HEAO-2 (Einstein) satellite in 1978, an imaging (<10 sec) and photometry (~1 nJy) capability comparable to those in the radio and optical wavebands.

Progress in experimental research utilizing dispersive techniques (e.g. Bragg and grating spectroscopy) has been considerably slower than that in areas utilizing photometric techniques, because of the relative inefficiency of the former for the weak X-ray signals from celestial sources. As a result, the term "spectroscopy" as applied to X-ray astronomy has traditionally satisfied a much less restrictive definition (in terms of resolving power) than it has in other wavebands. Until quite recently, resolving powers of order unity were perfectly respectable, and detectors with resolving power $R = E/\Delta E \lesssim 10$ still provide (in most cases) the most useful spectroscopic data.

In the broadest sense, X-ray photometric measurements are spectroscopic, insofar as they represent samples of the overall electromagnetic continua of celestial objects. The very detection of galactic X-ray sources, with luminosities $\gtrsim 10^{36}$ ergs/s, established their effective temperatures at $\gtrsim 10^7$ K even before they were individually identified. Rocket-borne proportional counter detectors with unit resolving power allowed data fits to simple spectral forms; the bremsstrahlung fit over 2-10 keV to the data from Sco X-1, for example, was extrapolated down to the optical to identify this brightest X-ray source in the sky with an undistinguished blue star (Sandage et al. 1966).

Improved proportional counters with R ≈ 7 in rocket-borne experiments measured the first X-ray emission lines (Fe-K at ~7 keV) from Cas A (Serlemitsos et al. 1973) and Cyg X-3 (Serlemitsos et al. 1975). Similar detectors flown on earth-orbiting satellites in the 1970's found Fe-K emission to be characteristic of many X-ray binaries (e.g. Pravdo 1979), as well as X-ray emitting supernova remnants and clusters of galaxies. With detector responses extended out to tens of keV this technology was able to characterize the X-ray continua of the diverse varieties of galactic X-ray sources over a dynamic range >10 (e.g. Holt 1980a).

The HEAO-1 spacecraft contained proportional counters large enough to interrogate fainter sources. Seyfert nuclei could now be studied in numbers sufficient enough to determine class properties, and their spectra turned out to be remarkably similar (Mushotzky et al. 1980). At higher energies (≳80 keV) some of the brighter active galactic nuclei were detected (e.g. Baity et al. 1981), with spectra consistent with extrapolation of their 2-50 keV spectral forms. The HEAO-1 experiments also investigated spectra at lower energies (i.e., down to ~100 eV) with ultra thin-window proportional counters, enabling the detection of lower temperature emission components (~10^6 K), in particular from stellar coronae and cataclysmic variables (e.g. Garmire 1979).

The second HEAO spacecraft, now known as the Einstein Observatory, provided qualitative breakthroughs in both photometric and spectroscopic X-ray astronomy (Giacconi et al. 1979a). Operating at relatively long X-ray wavelengths (~0.1-4 keV) because of its utilization of grazing incidence optics, the imaging capability of Einstein provided detection sensitivities a thousand times better than previously achieved. Almost every type of star in the galaxy became measurable in X-rays, and the catalog of X-ray quasars increased a hundred-fold from the 2 or 3 that were previously detectable. The array of instruments on Einstein included spectrometers with complementary attributes: a high-efficiency,

moderate resolving power (~15) photoelectric detector, and two lower efficiency dispersive instruments with much higher resolving power (~100). Both types have successfully detected emission lines.

The recent cessation of the operation of Einstein has created a temporary hiatus on the availability of new X-ray data in general, and new spectroscopic data in particular. This review takes stock of the current and anticipated near-term capabilities of X-ray spectroscopic instrumentation in terms of their application to the most pressing scientific issues.

B. Instrumental Considerations

Virtually all pre-Einstein X-ray spectroscopy has been performed with proportional counters, which have a resolving power limited to $R \sim 3(E/1\ keV)^{1/2}$ by the nature of the atomic interactions in the counter gas following the primary photoabsorption. The gas scintillation proportional counter (e.g. Peacock et al. 1980) promises to improve this resolving power by a factor of ~2. Higher resolving powers in nondispersive devices can be achieved by using semiconductors instead of gas as the detector medium. The most successful such instrument so far has been the Einstein SSS (solid state spectrometer), a cryogenically cooled silicon chip with resolving power $R \sim 6\ (E/1\ keV)$. Like other charge collecting proportional counters, the SSS has a photoelectric detection efficiency approaching 100%.

Dispersive devices, of which the Einstein FPCS (focal plane crystal spectrometer, with R ~ 60 to 700), and OGS (objective grating spectrometer, with R ~ 30), are prototypes for future instrumentation, and can be designed to have $R \sim 10^3$ or better at the expense of broadband efficiency. Such instruments will require substantially larger collecting areas to obtain useful signals from most sources.

Ordinarily we shall characterize X-ray spectra by F(E) in units of ergs cm^{-2} s^{-1} keV^{-1}; thus, power law spectra, $F(E) \propto E^{-\alpha}$, will be characterized by the energy spectral index, α, used conventionally in radio astronomy. The problem of translating from counts detected in a spectrometer to such a source spectrum is not trivial, and it is important to recognize that the interpretation of an observation depends on the procedure that is employed. The raw data are a convolution of the actual photon spectrum with the response function of the detector, but their inversion to a derived input spectrum is not unique. The conventional inversion (e.g., Holt 1980a), is a model-dependent procedure that requires the observer to have some a priori knowledge of the actual spectral form, so that its shape can be characterized by a limited number of adjustable parameters. Typical fitting parameters are amplitude and shape of continuum (usually characterized by a power law with a high energy exponential cutoff), strengths (and possibly energies) of emission lines and photoelectric absorption edges, and low energy photoabsorption by intervening cold matter (e.g., Fireman 1974). Simulated detector count spectra are computed from the assumed photon spectral forms, and the model parameters are varied to achieve the best fit to the actual detector counts. With this procedure, spectral features blurred by the detector response can be enhanced for display, as illustrated in Figure 1. The hazard of this procedure is that unanticipated features in the actual photon spectrum are forced to be represented by the model fitting parameters, so that, for example, an intrinsically broadened emission line might appear as a doublet if only sharp lines were anticipated, etc.

Model-independent inversion procedures exist that allow less subjective representations of the source spectrum (e.g., Holt 1980a), but a model must ultimately be employed in order to relate spectral features to parameters associated with physical processes.

II. OPTICALLY THIN THERMAL SOURCES

A. Physical Processes

In many astrophysical contexts, an X-ray-emitting plasma is sufficiently transparent that the emergent spectrum faithfully represents the microscopic emission process occurring in the plasma. At temperatures $T \gtrsim 10^8$ K, almost all abundant elements in a cosmic plasma are fully ionized, and the X-ray emission is dominated by bremsstrahlung from hydrogen and helium, giving a spectral emissivity $j(E) \propto n_e^2 E^{-0.4} \exp(-E/kT)$ ergs cm^{-3} s^{-1} keV^{-1} (Rybicki and Lightman 1979). However, at lower temperatures trace elements retain a few atomic electrons, and their contribution to the emissivity cannot be ignored. Because cross sections for electron impact excitation of such ions far exceed those for bremsstrahlung or radiative recombination, line emission from $Z \geq 8$ constituents actually dominates the cooling from plasma with $10^4 < T < 10^7$ K, even though these trace elements represent only $\sim 10^{-3}$ of the plasma composition by number.

A theoretical model is needed to infer physical parameters such as temperature, element composition, and density from the observed spectrum of an optically thin plasma (cf. McCray 1982). To construct such a model requires knowledge of the ionization state of each trace element, which is controlled by electron impact ionization and radiative and dielectronic recombination. If the plasma is maintained at constant temperature and density for a long time compared to the timescales for these microscopic processes, the ionization of trace elements relaxes to a stationary state that depends primarily on electron temperature and weakly on density. This stationary ionization balance assumption was first employed to interpret the solar, corona and many such "coronal models" have been calculated. The most recent calculations of the stationary ionization balance are those by Shull and Van Steenberg (1982), and of the X-ray emissivity are those by Shull (1981). An exemplary spectrum is shown in Figure 2.

Such spectra are rich in emission lines and offer the opportunity to deduce many properties of the emitting gas when sufficient resolving power and sensitivity are available. The main emission complexes from K_α transitions of helium-like and hydrogenic ions of abundant elements such as O, Ne, Mg, Si, S, Ar, Ca, and Fe become distinct with $R \gtrsim 10$. A temperature may be inferred from the relative strengths of the helium-like and hydrogenic lines from a given element, but its validity depends on that of the stationary ionization balance assumption. A measure of temperature independent of that model assumption may be obtained from ratios of K_β/K_α transitions of a single ion if there is sufficient sensitivity to measure the generally weak K_β feature. With $R \gtrsim 100$ a variety of more powerful temperature and density diagnostics become available. "Satellite lines" resulting from dielectric recombination appear with photon energies slightly less than those of the resonance lines, and may be used as temperature diagnostics (Dubau et al. 1981). The K_α complexes of helium-like ions break up into resonance (2^1P), intercombination (2^3P) and forbidden (2^3S) components, the relative strengths of which can be used to infer electron temperature and density (Pradhan and Shull 1981).

Coronal models may be used to infer the element abundances and electron temperatures of X-ray sources by fitting the theoretical models convolved through the detector response with the data as described in §I.B. With enough model parameters an acceptable fit to the data is virtually guaranteed. However, two important caveats must be kept in mind in interpreting these results. The first is that the derived parameters are valid only insofar as the model assumptions are correct; as we shall see in the remainder of this paper, such coronal models are inappropriate to most categories of celestial X-ray sources. The second caveat concerns the accuracy of the atomic physics that goes into the theory. Because few of the relevant atomic rate coefficients

are known experimentally, we must rely largely on theoretical calculations. Thus, abundance determinations based on X-ray emission line ratios are no more accurate than the approximate theoretical rate coefficients for the emitting ions, which may differ from the true rates by factors ~3.

B. Intergalactic Gas in Clusters

Perhaps the best astrophysical application of the coronal model is to clusters of galaxies (Bahcall and Sarazin, 1978). Here the transparency of the gas to its own radiation is assured (i.e., $\tau_o = \sigma_T n_e R \lesssim 10^{-3}$), and the dynamical timescale of the gas approaches 10^9 years, much longer than the characteristic recombination timescale.

The X-ray spectra of all clusters are dominated by bremsstrahlung with $T \sim 10^8$ K (Mushotzky et al. 1978a), which must certainly arise in a hot intergalactic gas. Recent X-ray imaging data from Einstein have confirmed the diffuse nature of the emission from clusters (Forman and Jones 1982), although individual galaxies (especially giant galaxies near the cluster centers) contribute to the X-radiation as well. The temperature of the dominant spectral component correlates with the traditional measures of the cluster gravitational potential: the velocity dispersion of galaxies (but cf. Sarazin 1982), and the central galaxy density (Smith et al. 1979).

The discovery of Fe-K-emission with proportional counters provided a crucial clue to the origin of the cluster gas. Because the coronal spectroscopic model should be appropriate to first order, the uncertainty in the inferred abundance should be limited by the atomic physics rather than the precision of the fit to the data. Virtually all clusters (e.g., Fig. 1) yield fits requiring an Fe abundance of approximately half-solar (referred to hydrogen), which implies that the cluster gas must have been processed through stars, and

removed from the galaxies by the action of supernovae or by ram-pressure-stripping as the galaxies passed through the intracluster gas (Sarazin 1982).

While an isothermal idealization of the cluster gas adequately describes the two most pronounced spectral features, i.e., the $\sim 10^8$ K continuum and the Fe-K emission, the physical situation requires closer examination. Gas this hot and rarefied radiates very inefficiently, so that an adiabatic approximation to the cluster gas in the gravitational potential of the cluster might be more appropriate. Polytropic models with arbitrary index generally cannot fit the X-ray data better than isothermal models, but interesting fits can be obtained if the polytropic index is allowed to be a function of distance from the center (e.g. White and Silk 1980).

The most significant departure from an isothermal spectrum is a low-energy excess, generally more pronounced in the more centrally condensed clusters, which can be fitted with a lower-temperature isothermal component. The cluster models of Cowie and Binney (1977), Fabian and Nulsen (1977) and Mathews and Bregman (1978) all infer increased cooling in the cluster cores as a result of the increased density, providing a possible explanation for the low-energy excess observed in proportional counter cluster spectra. The discovery of O VIII emission from M87 with the Einstein FPCS validated the identification of this low energy excess with a lower-temperature component (Canizares et al. 1979). Einstein SSS cluster data require Si XIII and S XV lines with the appropriate cluster redshift in order to achieve formally acceptable fits (Holt 1980b). The data are generally not good enough to require a model more refined than two isothermal components.

Typically, the emission measure in the dominant high temperature component represents a hot gas containing ~10% of the cluster virial mass, and the cooling region has an emission integral <10% of the high temperature component. If we

assume pressure equilibrium between a central isothermal component and the surrounding hotter cluster gas, the SSS data from the Perseus cluster give a core size of ~10 kpc and cooling time of $\sim 10^9$ yr; it is interesting to note that the former is consistent with the "stagnation radius" in the Cowie and Binney model, and the latter implies that the mass of NGC 1275 can be accumulated by such accretion at the cluster center over a Hubble time (Mushotzky et al. 1981a).

C. Stellar Coronae and Winds

The X-ray photographs from Skylab of the solar corona demonstrated that the solar X-ray emission did not arise in a homogeneous corona, but was instead confined to loop structures. This was true for the relatively quiescent coronal emission as well as that associated with solar flare active regions. The loop structures appeared to satisfy a relation derived by Rosner, Tucker and Vaiana (1978) for the maximum extent into the corona, L, of the loop above its footpoints in the transition region. In the limit where L is small compared to a pressure scale height, $L \approx 5\ T_7^3\ p^{-1}$, where L is measured in solar radii, T_7 in units of 10^7 K, and p in dynes cm^{-2}.

The discovery of X-ray emission from RS CVn variables with the HEAO-1 proportional counters (Walter et al. 1980) provided a natural application for this model. The active components of RS CVn systems are somewhat later in spectral type than the Sun, and show optical flare-active regions which approximately co-rotate with the binary period of the system (Hall 1976). The similarity to solar flare active regions and the observed $\sim 10^7$ K temperatures (far exceeding the escape velocities of the stars) virtually demand magnetic confinement for the X-ray-emitting plasma.

X-ray spectral measurements by the Einstein SSS validated the coronal model assumptions with the measurements of Si and S K-emission and Fe L-

emission from Capella having near-solar abundances (Holt et al. 1979); the measurements generally required two temperature components for an adequate fit to the spectra of late stars in binary systems (Swank et al. 1981). Interestingly, the eight systems reported by Swank et al. could all be fit with components $T \lesssim 10^7$ K and $T \sim 10^8$ K, but the relative emission measures in the two components varied considerably from system to system. For typical pressures, the lower temperature component correlated reasonably well with active regions confined to the stellar surface, while the higher temperature component was consistent with loop structures connecting the two components of the binary system (Swank et al. 1981).

Einstein has now observed X-ray emission from stars with positions all over the H-R diagram (except for red giants; see Vaiana et al. 1981). Soft X-ray emission ($\log T \sim 6.5$) has been detected from many Of stars and OB supergiants, with $L_X/L_{BOL} \sim 10^{-7.5}$ (Long and White 1980; Pallavicini et al. 1981; Cassinelli et al. 1981). Such stars have strong, relatively cool ($\log T \lesssim 4.5$) stellar winds. That these stars might be X-ray sources had been predicted (Cassinelli and Olson 1979) in order to explain the presence of highly ionized species such as O VI in their UV spectra. The X-ray temperatures are typically too low to exhibit emission features to which the Einstein SSS is sensitive, but the absence of soft X-ray cutoffs in the spectra (Stewart and Fabian 1981) shows that the X-ray source cannot be a corona located at the base of the wind, but instead must have components distributed throughout the wind (Cassinelli and Swank 1982).

D. Supernova Remnants

Supernova explosions are believed to be the primary mechanism for the production and dispersal of heavy elements into the interstellar medium (ISM) and for the origin of cosmic rays (Shklovsky 1968). They also play a major

role in the dynamics of the ISM (McCray and Snow 1979). The quest to understand these processes has driven the development of research in many areas of astronomy, including X-ray spectroscopy.

Excluding sources like the Crab Nebula, which contains a powerful non-thermal energy source in its interior, most supernova remnants (SNR) have a shell-like X-ray morphology that can be approximated in terms of a spherically symmetric blast wave (Sedov 1959; Taylor 1950). In this idealized model a supernova explosion ejects a few solar masses with kinetic energy 10^{51} E_{51} ergs into a homogeneous interstellar medium with atomic density n_o (cm^{-3}). After a few centuries the mass of the shocked interstellar gas exceeds that of the ejecta, and the radius of the blast wave is given by $R \approx 5.1(E_{51}/n_o)^{1/5}\ t_3^{2/5}$ pc, where $t_3 = t/10^3$ yr. The gas is compressed to $n \sim 4\ n_o$ in a shell of thickness $\sim$ 0.1 R, and the post-shock ion kinetic temperature is given by $kT_i \approx 10(E_{51}/n_o)^{2/5}\ t_3^{-6/5}$ keV.

Heiles (1964) calculated the bremsstrahlung X-ray continuum spectrum from such a blast wave. Tucker (1970) recognized that the emission would be dominated by lines, and calculated broad-band X-ray emissivities of SNR by assuming that the shocked gas radiated with a spectrum appropriate to a gas in coronal ionization equilibrium. Since the timescales for the dominant ions in the shocked gas to reach equilibrium exceed the ages of young SNR, realistic models for their X-ray emission spectra require simultaneous solution of many detailed ionization rate equations along with the hydrodynamical equations. Moreover, the timescale for electron-ion temperature equilibration by Coulomb collisions (Spitzer 1962) may be long enough that $T_e < T_i$, unless plasma instabilities reduce the equilibration timescale (McKee 1974).

Recently, several authors (Itoh 1977,1978,1979; Gronenschild and Mewe 1982; Shull 1982) have constructed detailed models demonstrating that departures

from ionization equilibrium can have dramatic effects on the X-ray spectra of SNR. Therefore, accurate determination of element abundances in SNR will require the incorporation of such departures into the analysis of their X-ray spectra. Generally, in a SNR the elements will be less ionized at a given electron temperature than the coronal models imply; as a result, the intensities of the dominant X-ray emission lines from helium-like ions will be enhanced, increasingly so with increasing atomic number.

The Einstein SSS data from the young remnants Cas A, Tycho (Fig. 2), and Kepler (Becker et al. 1979a,1980a,1980b) show clear evidence for departures from ionization equilibrium. In each case the observed ratios of hydrogenic to helium-like lines of Si and S imply ionization temperatures $kT_z \sim 0.5$ keV, while fits to the >3 keV continuum require electron temperatures $kT_e \gtrsim 4$ keV. This multiplicity of temperatures may result in part from a substantial additional contribution to the emission from cooler reverse-shocked supernova ejecta (McKee 1974; Itoh 1977, 1978, 1979; Chevalier 1982), and in part from departures from ionization equilibrium. Pravdo and Smith (1979), using proportional counter data from HEAO-1, measured X-ray continuum spectra of Cas A and Tycho to ~25 keV, implying electron temperatures kT ~ 10 keV and suggesting more rapid electron-ion temperature equilibration than possible via Coulomb collisions alone.

Abundances (relative to hydrogen) of the elements Si, S, Ar, and Ca inferred from fits of coronal equilibrium models to the SSS data from Cas A, Tycho, and Kepler exceed the solar values by substantial factors. For example, the inferred enhancements of Si/H are ~2 in Cas A, ~4 in Kepler, and ~6 in Tycho, and the enhancements of S, Ar, and Ca are progressively greater. On the other hand, the ratios Fe/H inferred from the L-blend emission near 1 keV are even less than the solar value. The progressive increase of the

enhancements of Si, S, Ar, and Ca inferred from K emission lines may be an artifice of the coronal equilibrium model. Indeed, this effect vanishes when the SSS data for Tycho are fit by Sedov blast wave models, in which the ionization is calculated from non-equilibrium rate equations (Shull 1982; Szymkowiak et al. 1982). Unlike the coronal equilibrium models, the non-equilibrium models can fit both the line and continuum data without requiring two separate temperature components. The abundances of Si, S, Ar, and Ca inferred in this way are still enhanced (by factors ~3-8) over the solar values, while the ratio Fe/H inferred from the L-blend is twice solar. The inferred ratio of Fe/Si in Tycho is still <1, however.

The combination of enhanced Si/H and low Fe/S observed in the young SNR's Tycho and Kepler is puzzling in view of theoretical models suggesting that a type I supernova explosion should eject a substantial fraction of a solar mass of Fe-group material (Colgate and McKee 1969; Arnett 1979). If the Si enhancement in young SNR is due to mixing of the supernova ejecta with the X-ray emitting plasma, similar mixing of Fe should yield Fe/Si > 10 (Smith 1981).

The X-ray images of some SNR are complex, clearly indicating propagation into an inhomogeneous ISM (McKee and Ostriker 1977). Multiple shock velocities and temperatures are likely; in Cas A, for example, the $kT_e \sim 1.5$ keV inferred from the ratio of the K_β/K_α emission features of Fe is much less than the $kT_e \sim 10$ keV inferred from the high energy continuum (Pravdo and Smith 1979), but greater than the $kT_z \sim 0.5$ keV inferred from the Si XIII/Si XIV ratio. Therefore, accurate abundance determinations in SNR will require more sophisticated hydrodynamical models and observations with higher spectral and spatial resolution.

For SNR older than $\sim 10^4$ yr, the nonequilibrium effects are much less severe, as evidenced by single temperature equilibrium fits to the SSS data

without the necessity of pronounced abundance anomalies. In one such case (the bright knot of emission northeast of the center of Puppis A), the intensity is sufficient for the Einstein FPCS to perform a complete scan for line emission in the range 0.5-1.1 keV with $E/\Delta E \sim 100$ (Winkler et al. 1981). A portion of this scan is displayed in Figure 3, illustrating the ability of the FPCS to resolve the helium-like resonance, intercombination, and forbidden lines that are blended together in the SSS data. The dominance of the resonance line over the intercombination line verifies that the ionization is collisional, as recombination would enhance the triplet transition. In addition, temperature and abundance diagnostics can be obtained from line ratios of both individual and separate ions of the same constituent; FPCS measurements of O VII and O VIII yield consistency with $kT \sim 0.2$ keV in Puppis A. Even if the plasma is not in equilibrium, relative element abundances can be inferred by comparing line ratios from ions of different species with line ratios from the same species, using the same ratios in the spectra of solar-active regions as a guide.

III. OPTICALLY THICK THERMAL SOURCES

A. Physical Processes

1. General considerations

One of the most exciting prospects of X-ray spectroscopy is the opportunity to elucidate the extreme physical environments associated with compact objects, ranging from galactic binary systems to active galactic nuclei (AGN). The rapid time variability observed from these sources indicates that they are very compact, with scale sizes $R < c\Delta t$ ranging from $\lesssim 10^7$ cm for the case of Cyg X-1 to $\lesssim 10^{13}$ cm for at least one AGN (NGC 6814). It is now certain that many compact galactic X-ray sources are white dwarf stars and neutron stars

and it seems likely that Cygnus X-1 and AGN contain black holes. In all these cases the X-ray luminosity derives from the release of gravitational energy by accreting matter. Gas flows in such systems are likely to be optically thick. Therefore, the X-ray spectrum we observe will contain information not only on the primary energy source, but also on the gas flow that feeds it. It follows that the interpretation of the observations will require an understanding of how X-ray spectra are modified by passage through an optically thick medium.

The luminosity that results from the accretion of gas at a rate $\dot{M}$ onto a compact object of mass M and radius R may be written $L \approx \eta c^2 \dot{M}$, where $\eta \approx GM/Rc^2$ is approximately $\eta \sim 3 \times 10^{-4}$ for a white dwarf star, $\eta \sim 0.1$ for a neutron star, and up to $\eta \sim 0.3$ for an accretion disk around a black hole (Thorne 1974). If the gas flow is steady and spherically symmetric, the emergent luminosity should not exceed the Eddington limit, at which the outward force on the accreting material due to Compton scattering balances the gravitational attraction: $L_E \approx 1.3 \times 10^{38}\ (M/M_\odot)$ ergs s^{-1}. The Compton optical depth is given by $\tau_o \gtrsim (2/\eta)^{1/2}\ L/L_E$, where the lower limit represents the case of spherically symmetric accretion. With non-spherically symmetric accretion flows, the steady-state luminosity may exceed L_E, but it is hard to invent source models for which $L \gtrsim 10\ L_E$.

There are two natural temperatures characteristic of accretion flows: the free-fall temperature, T_{ff}, and the black-body temperature, T_{BB}. The former is very high: $kT_{ff} \approx \frac{3}{16}\ \eta\ m_H c^2 \approx 2 \times 10^5\ \eta$ keV, which gives $kT_{ff} \sim 50$ keV even for a white dwarf. The latter is the minimum temperature required for the source to radiate the observed luminosity: $T_{BB} \approx (L/A\sigma_s)^{1/4}$, where A is the radiating surface area and σ_s is the Stefan-Boltzmann constant. The Eddington limit sets an upper limit on T_{BB} which is generally much less than T_{ff}: $kT_{BB} \lesssim 0.2$ keV for a white dwarf, $kT_{BB} \lesssim 2$ keV for a neutron star, and $kT_{BB} \lesssim 1$ keV $(M/M_\odot)^{-1/4}$ for

a black hole. The characteristic temperature of the radiation produced by a compact source usually falls between T_{ff} and T_{BB} and may be determined by some other natural energy such as the excitation energy of atomic or cyclotron lines. For a given source mass, the spectral temperature is likely to be lower at higher luminosity, for which the accretion flow will be more opaque and will effectively soften the radiation.

2. Nebular models

The photoelectric opacity at 1 keV of a gas of normal cosmic abundance exceeds the Compton opacity by a factor of ~400 if the oxygen ions are not fully stripped. Therefore, there is a substantial range of column densities for which a distribution of gas may be opaque to photoelectric absorption but transparent to Compton scattering: this is the nebular approximation. A point source of continuum X-rays surrounded by such a distribution of gas is the X-ray analogue of a planetary nebula. The ionization and temperature of the surrounding gas are controlled by photoelectric absorption and line emission by the gas, and the emergent spectrum gains atomic absorption and emission features as a result of propagating through the gas. Models for X-rays incident on a one-dimensional slab, used to represent quasar emission line regions, have been reviewed by Davidson and Netzer (1979); the most recent such calculations are those by Kwan and Krolik (1981). The most recent models for a point source of X-rays surrounded by a spherically symmetric gas cloud are those by Kallman and McCray (1982).

The results of such calculations are the temperature and ionization of the elements as functions of the distance from the X-ray source, and the emergent spectrum. Generally, the gas becomes progressively cooler and less ionized further from the source as a result of photoelectric absorption (in slab models)

and geometrical dilution (in spherical models) of the primary radiation. If the X-ray spectrum is not too soft ($\alpha \lesssim 2$), the gas nearest the X-ray source is maintained at a high temperature, $kT \sim E_{max}/4$, as a result of Compton scattering by the hardest (E_{max}) photons in the source spectrum. At greater distances, cooling due to atomic emission lines becomes important and the temperature drops to $T \sim 10^4$ K. This transition, which is almost discontinuous in constant pressure models, may account for the distinction between cool clouds and the hot intercloud medium in AGN (McCray 1979; Krolik et al. 1981). The ionization structure is dominated by photoionization rather than electron impact ionization. Therefore, at a given temperature the elements are more highly ionized in the nebular model than in the coronal model, and the more so if the source spectrum is soft. Auger ionization is important and can produce several ionization stages of trace elements at the same place. For a given source spectrum the temperature and ionization are functions only of the column density of gas to the source and of an "ionization parameter," proportional to the X-ray flux divided by the gas density.

As the X-rays propagate into the nebula, a photoelectric absorption cutoff appears in the continuum spectra, first at soft X-rays and then at progressively higher energies. The absorbed luminosity is reemitted by the gas as emission lines and continuum recombination radiation. Typically, the strongest X-ray emission lines appear at photon energies near the soft X-ray cutoff. If the nebula is thick enough these secondary X-ray emission lines are also photoabsorbed, and ultimately most of the absorbed X-ray luminosity is converted to UV emission lines ($E < 13.6$ eV), such as L_α, He II λ1640, C IV λ1540, and O VI λ1035, which can escape the nebula. Resonant trapping of emission lines can have important effects on the temperature of the emission line region and on the emergent spectrum.

A particularly important diagnostic of gas photoionized by X-rays is the complex of emission lines at 6.40-6.67 keV due to K-fluorescence of iron (Fe I-Fe XXIV). Iron is unique among the cosmically abundant elements in having a high ($Y_K \approx 30\%$) fluorescence yield following photoionization of a K electron (in contrast, C, N, O, Si, S have $Y_K < 3\%$). Comparison of the strength of the fluorescence feature with that of the K-photoabsorption for $E > 8$ keV can provide valuable information on the geometry of the gas around a compact source, since the photoabsorption is produced along the line of sight to the primary source, while the fluorescence line is produced by all the gas that is illuminated by the source (Pravdo 1979).

3. Comptonization

Compton scattering dominates the photoelectric opacity of a plasma of solar system composition for photons with $E \gtrsim 10$ keV in general, and for lower photon energies if the electron plasma is hot enough ($T_e \gtrsim 10^7$ K) such that abundant elements such as He, C, and O are fully ionized. As a result of the electron recoil, photons of initial energy E_o undergoing multiple scattering in an electron gas of temperature T_e tend to equilibrate, so that hard photons ($E_o > kT_e$) lose energy to the gas and soft photons gain energy. Because of its importance to X-ray astronomy, the theory of this "Comptonization" has undergone considerable development during the past few years (Rybicki and Lightman 1979; Illarionov et al. 1979; Sunyaev and Titarchuk 1980).

After a mean number of scatterings, u, a spectral line will have a mean energy shift $\Delta E \approx uE_o(4\ kT_e - E_o)/m_ec^2$ and line width $\delta E \approx u^{1/2}\ E_o\ (\frac{7}{5} E_o^2 + 2kT_e m_e c^2)^{1/2}/m_e c^2$. The resulting line profiles have considerable structure depending on the geometry of the scattering region; methods for calculating the profiles and a variety of examples have been

described by Basko (1978), Pozdnyakov et al. (1979), Illarionov et al. (1979), and Langer (1979).

When the number of scatterings is large, the development of the spectrum is described by an energy-diffusion (Fokker-Planck) equation, first derived by Kompaneets (1957). This equation has as its stationary solution a Bose-Einstein spectrum, $I(E) \propto E^3[\exp(E + \mu)/kT_e - 1]^{-1}$. This equilibrium spectrum is not necessarily Planckian ($\mu = 0$), because Compton scattering preserves the number of photons. The Kompaneets equation is approximate and does not accurately describe the development of the spectrum in every case. In particular, it must be modified when the electron temperature is much less than the photon energy (Ross et al. 1978; Illarionov et al. 1979), and it fails for gas temperature or photon energy exceeding $\sim 0.1\ m_e c^2 \sim 50$ keV. Guilbert (1981) has developed an integral equation suitable for the latter situation.

The development of the spectrum in an actual situation is governed by an equation that accounts for the effects of both spatial and energy transfer. A few special cases are of particular interest:

a) Source of cool photons surrounded by hot electrons. Such models have been proposed to represent spectral formation in compact binary systems (Shapiro et al. 1976) and active galactic nuclei (Katz 1976). In this case the emergent spectrum develops a high energy tail whose form is independent of the source spectrum but depends on the optical depth, τ_o, of the electron distribution. The mean number of scatterings is $u \approx \tau_o^2/2$. The shape of the spectrum is governed by the Comptonization parameter, $y \equiv 4kT_e\ u/m_e c^2$. For $y \gg 1$ or $E > kT_e$ the spectrum will have the Wien form, $I(E) \propto E^3 \exp(-E/kT_e)$. For $y \lesssim 1$ and $E < kT_e$ the spectrum will have a power law form $I(E) \propto E^{-\alpha}$ where $\alpha = -\frac{3}{2} + \left(\frac{9}{4} + \frac{4}{y}\right)^{1/2}$. Sunyaev and Titarchuk (1980) have derived more general analytical expressions for I(E). Note that a thermal distribution of hot electrons can cause the

formation of an emergent spectrum that resembles the power-law spectrum resulting from synchrotron radiation or inverse Compton scattering by a non-thermal power-law distribution of relativistic electrons (§IV).

The power of the radiation source is amplified substantially by Comptonization when $y \gtrsim 1$. Shapiro et al. (1976) and Liang (1979) have suggested that the resulting energy losses of the electron cloud will act as a thermostat, such that y will remain close to 1. If so, the emergent spectrum will approximate a power law with $\alpha \approx 1$, as seems to be the case for active galactic nuclei.

b) Source of hot photons surrounded by cool electrons. In this case the photons are scattered to lower energy by the electrons and the emergent spectrum will develop a high-energy cutoff at $E_{max} \approx \max\{kT_e, 2m_e c^2/\tau_o^2\}$. No analytic expression is known for the shape of the high-energy spectrum; numerical results have been calculated by Ross et al. (1978), and by Langer et al. (1978).

c) External source of cool photons reflecting from a semi-infinite slab of hot electrons. This case has been solved by Lightman and Rybicki (1979a,b). The resulting spectrum is a universal function, $I(E) \propto (\ln E/E_o)^{-3/2}$ for $E < kT_e$ and $I(E) \propto E^3 \exp(-E/kT_e)$ for $E > kT_e$, which may be hard to distinguish from optically thin bremsstrahlung. Lightman, Lamb and Rybicki (1981) have obtained results for sources of hot photons internal and external to a semi-infinite slab of hot electrons.

d) Temporal variability. Interesting time-dependent effects may occur if the photon source is variable (Lightman and Rybicki 1979b; Payne 1980). If the photon source is hotter (or cooler) than the ambient electrons, the Comptonized spectrum becomes progressively softer (or harder) following an impulsive outburst; the timescale for the spectral reverberation provides additional information on the geometry of the ambient gas.

e) Compton heating/cooling. The electron gas is heated or cooled as it Comptonizes the photons propagating through it (Rybicki and Lightman 1979). If the energy density of the radiation exceeds that of the thermal electrons and the Compton heating/cooling timescale is less than other dynamical timescales, the electron temperature will be slaved to an effective temperature, T_{eff}, of the radiation field, where $T_{eff} \approx T_{rad}$ for a dilute Planck or Wien radiation field and $kT_{eff} \approx E_{max}/4$ for an exponential or power law spectrum with energy spatial index $\alpha < 2$ and upper cutoff energy E_{max}. When the radiation field has a strong soft X-ray or UV excess (or $\alpha \gtrsim 2.5$), Comptonization actually drives the electron temperature toward the lowest photon energy, E_{min}.

4. Diffusion models

In general, the X-ray spectrum resulting from the reprocessing of the primary source spectrum by an optically thick distribution of gas will be formed by the combined effects of atomic emission and absorption and Comptonization. The X-ray albedo and iron line fluorescence of a cold stellar atmosphere have been calculated by Basko et al. (1974), Felsteiner and Opher (1976), Basko (1978) and Bai (1979). Models for the transfer of X-rays through an optically thick spherically symmetric shell including Comptonization and atomic processes have been calculated by Ross (1979).

B. Accreting White Dwarf Stars

There are many known binary systems in which mass transfer is occurring from a late-type star onto a white dwarf star. These are the cataclysmic variable stars, including classical novae, recurrent novae, dwarf novae, and related systems (Robinson 1976). A number of these systems have been detected as X-ray sources (Cordova, Mason and Nelson 1981), but most are so faint

(F_x(1-4 keV) $\lesssim 10^{-11}$ ergs cm^{-2} s^{-1}) that not much is yet known about their spectra except that they are fairly hard ($kT \gtrsim 10$ keV). We shall briefly summarize the models and recent observations; a more detailed account and further references can be found in the review by Kylafis et al. (1980).

The accreting white dwarf stars can be divided into two main classes: (1) those showing features in their optical and UV spectra and light curves that clearly indicate an accretion disk; and (2) those showing evidence of very strong ($\sim 10^7$ G) magnetic fields — sufficient to prevent the formation of an accretion disk. The magnetic dwarfs will be discussed in §V. Two kinds of theoretical models have been proposed to describe the X-ray emission from the non-magnetic systems: (1) spherically symmetric radial accretion; and (2) an accretion disk extending to the white dwarf surface (Pringle 1981).

Model (1), spherical accretion, may be so idealized that it has no actual counterparts, but it has the virtue that it may be solved in sufficient detail to provide many valuable insights. The most recent such calculations are those by Kylafis and Lamb (1979, 1982) and Ross and Fabian (1980). The infalling gas forms a shock above the surface of the white dwarf. At low accretion rates the shocked gas radiates very inefficiently and the shock stands high above the surface, but as the accretion rate increases the thickness of the cooling layer decreases and the shock moves near the surface. In either case the X-ray emission comes primarily from gas with $T \sim T_{ff}$. Half the X-ray emission propagates outward through the accreting envelope; the other half propagates downward and is re-radiated as blackbody radiation at T_{BB} by the white dwarf surface. The blackbody luminosity, L_{BB}, of the white dwarf surface may be some 60 times greater than that due to the intercepted X-ray luminosity if steady thermonuclear burning of the accreting gas ensues, but such burning is more likely to be sporadic.

When the accretion rate is low ($L_{TOT} \lesssim 10^{36}$ ergs s^{-1}) the envelope is fully ionized and optically thin to the X-ray emission. In that case, the accretion luminosity will have a spectral shape almost independent of L_{TOT}, consisting of optically thin X-ray bremsstrahlung with $kT_X \sim 50$ keV, and a blackbody with $kT_{BB} < 0.1$ keV. When $L_{TOT} \gtrsim 10^{36}$ ergs s^{-1}, the accretion flow becomes optically thick and the emergent spectrum is modified considerably by Comptonization and photoelectric absorption as it propagates through the flow. The result is that the X-ray photons are degraded to lower energy and that the hard X-ray luminosity actually decreases with increasing L_{TOT}, giving a maximum hard X-ray luminosity $L_H \sim 4 \times 10^{36}$ ergs s^{-1}. The suggestion by Kylafis and Lamb (1979) that Cygnus X-2 might be an accreting white dwarf displaying this behavior seems to be ruled out by its large (~8 kpc) distance (Cowley et al. 1979), implying $L_H \approx 10^{38}$ ergs s^{-1}.

Many of the cataclysmic variables that have been observed as X-ray sources show clear evidence of accretion disks. During quiescent periods they have typical X-ray luminosities $L_X \sim 10^{30}$–10^{31} ergs s^{-1} and spectral temperatures $kT \sim 5$–20 keV. Two important examples, SS Cygni and U Gem, have also been observed during optical outburst (Cordova et al. 1981; Fabbiano et al. 1981). At those times a very soft blackbody component ($kT \sim 20$–30 eV) appeared in the X-ray and UV spectrum with luminosity $\gtrsim 10^2 L_X$. The soft X-rays displayed quasi-periodic oscillations with timescales ~10 s. These systems are obviously complex and detailed models for the formation of their X-ray spectra do not exist. Pringle and Savonije (1979) suggest that the hard X-rays come from a boundary layer between the accretion disk and the white dwarf star, where the accreting gas is heated to X-ray temperatures by some sort of shock as it is slowed from the Kepler velocity of the disk to the rotational velocity of the star. The disk is likely to be opaque to X-rays if the accretion rate is high, so that much of

the hard X-ray luminosity generated in the boundary layer may be absorbed and reemitted at much lower temperatures. Fabbiano et al. (1981) suggest that the soft X-rays during outburst may result from a thermonuclear flash.

C. Accreting Neutron Stars

1. General Characteristics

There are ~100 luminous ($L_x \sim 10^{36} - 10^{39}$ ergs s^{-1}) compact X-ray sources in the Milky Way and Magellanic Clouds, of which ~55 have known optical counterparts (Bradt and McClintock 1982). Excluding the isolated Crab and Vela pulsars, 19 are pulsating sources with periods ranging from 0.71s (for SMC X-1) to 835s (for X-Per, which has an anomalously low luminosity $L_x \sim 10^{34}$ ergs s^{-1}). The pulsation periods have been observed to generally decrease over characteristic timescales ranging from ~100 yr to ~10^6 yr, and the relationship between the derivative of the pulse period and the X-ray luminosity clearly indicates disk accretion onto a magnetized neutron star of mass ~1-3 $M_\odot$ (Ghosh and Lamb 1979; Elsner et al. 1980a; Rappaport and Joss 1982). Most (~15) of the X-ray pulsars are known to have massive ($\gtrsim 8\ M_\odot$) OB companion stars. Only two are known to have relatively low mass companions: Her X-1 (~2 $M_\odot$) and 4U 1626-67 (~0.1 $M_\odot$).

Of the remaining luminous sources that do not pulse, most have faint (if any) optical counterparts and are low-mass systems concentrated toward the galactic bulge with a Population II distribution. A few (~10) have orbital periods determined from X-ray or optical photometry, or optical spectroscopy [e.g.: Sco X-1 (18.9^h), Cyg X-2 (9.8^d), Cyg X-3 (4.8^h) and 4U 1822-37 (5.57^h)]. The rest, which include persistent galactic center sources, transients, and X-ray burst sources, have no known periodicities. Their high X-ray/optical luminosity ratios, in particular, lead us to believe that most of these sources are also accreting neutron stars in binary systems.

The following system structures are likely to produce direct effects on the X-ray spectra (McCray 1977): a stellar wind from the companion star; a gas stream from the companion star that feeds an accretion disk; the disk itself; a possible hot corona or wind from the disk; the "Alfven surface," where the disk is disrupted by the magnetosphere of the neutron star; and finally, the primary emitting region where the accretion flow encounters the neutron star surface. In this section, we shall try to elucidate these effects with examples from specific sources and to show how their interpretation might provide a basis for modeling the geometries of individual systems.

Figure 4 shows the spectrum of the 1.24[s] pulsating binary X-ray source Her X-1, which has a maximum luminosity (averaged over pulsations and assuming an isotropic source) $L_X \sim (2 \times 10^{37}$ ergs $s^{-1})(D/6$ kpc$)^2$. Most of this luminosity appears in a flat ($\alpha \approx 0$) power law continuum with a break at $E_{max} \approx 20$ keV, above which $\alpha \gtrsim 3$. Other prominent features in the time-averaged spectrum are: (1) a strong soft X-ray excess, containing about 15% of the luminosity, that may be fit with a blackbody with kT ≈ 0.11 keV; (2) a broad (FWHM ~ 2.4 keV) iron K-fluorescence line at ~6.4 keV with an equivalent width E.W. ~ 0.3 keV (Pravdo et al. 1977); and (3) a feature at ~55 keV, containing about 2% of the luminosity. The 55 keV feature and the pulse-phase dependence of the hard X-ray spectrum probably result from processes occurring at the surface of the highly magnetized neutron star; they are discussed in §V.

In many respects, the spectrum of Her X-1 is typical of the pulsating binary X-ray sources. Almost all of them have a hard ($\alpha \approx 0.2 \pm 0.4$) approximately power law continuum (e.g., Rappaport and Joss 1982) a spectral break ($10 < E_{max} < 30$ keV), and a broad 6.4 keV iron line ($0.2 \lesssim$ E.W. $\lesssim 0.7$ keV) (Pravdo 1979). The only exception is the subluminous source X-Per, which has an exponential spectrum with kT ~ 12 keV and no iron line (Becker et al. 1979b).

2. Magnetospheric Gas

A simple blackbody argument shows that the soft X-ray flux from Her X-1 cannot come from the neutron star surface but must come from a distance $R \gtrsim 10^8$ cm. Evidently ~15% of the hard X-ray luminosity is intercepted there and reradiated at $kT \sim 0.11$ keV by a partially opaque distribution of matter. McCray and Lamb (1976) and Basko and Sunyaev (1976) pointed out that $R \sim 10^8$ cm has dynamical significance, nearly coinciding with the corotation radius and Alfven radius where one might expect accreting matter to pile up. It is likely that the iron fluorescence lines come from the same distribution of matter responsible for the soft X-rays. The width of the iron line, which appears to be broader than instrumental (with $R \sim 7$), may result from Doppler motions of the reprocessing matter or from Comptonization. Ross et al. (1978), Ross (1979), Basko (1980), and Bai (1980) have discussed models for the reprocessing of hard and soft X-rays and iron line formation by matter at this "Alfven shell" of Her X-1; however, there is clearly much work to be done to gain a proper understanding of this region. In particular, we need to understand the source geometry that causes the maximum of the 1.24^s soft X-ray pulse (cf. Fig. 4) to lag the hard X-ray pulse maximum by $\Delta\phi \sim 0.6$ (McCray et al. 1982).

A similar soft X-ray excess is seen in the spectrum of SMC X-1 (Bunner and Sanders 1979) but without the phase lag. Unfortunately, interstellar absorption prevents us from knowing the soft X-ray spectra of most galactic binary sources. In these cases, the fluorescent lines may be the only spectral diagnostics of the magnetospheric gas.

3. Stellar Winds

Several binary X-ray systems have luminous OB companion stars (Bradt and McClintock 1982), which typically have strong stellar winds with mass loss

rates $\sim 10^{-7} - 10^{-5}$ $M_\odot$ yr^{-1} and terminal velocities ~1000-3000 km s^{-1} (Conti and McCray 1980). Buff and McCray (1974) pointed out that such winds have sufficient column density to cause significant soft X-ray absorption that should vary in a predictable way with X-ray orbital phase, and Hatchett and McCray (1977) showed how to calculate the ionization structure and soft X-ray absorption in a binary source embedded in a strong spherically symmetric stellar wind. Stellar winds are likely to account for the increase in absorption observed near eclipse in the spectra of Cen X-3 (Pounds et al. 1975; Schreier et al. 1976), 4U 1700-37 (Mason et al. 1976), Vela X-1 (Becker et al. 1978a; Charles et al. 1978), and possibly GX301-2 (Swank et al. 1976). Hertz et al. (1978) have made Monte Carlo simultations of X-ray transfer through stellar winds, and have suggested that electron scattering may account for the residual intensity observed during eclipse of Cen X-3 and Vela X-1.

The embedded compact X-ray source is likely to substantially modify the dynamics of the wind. Gravitational focusing of the flow can cause an accretion wake (Illarionov and Sunyaev 1975; Wolfson 1977; Carlberg 1978), X-ray heating or radiation pressure can cause a bow shock (Krasnobaev and Sunyaev 1977), and X-ray ionization can modify the radiative acceleration of the stellar wind (Hatchett and McCray 1977; Fransson and Fabian 1980). It has been suggested that such structures might be responsible for photoelectric absorption dips observed near superior conjunction in Cen X-3 (Jackson 1975) and Vela X-1 (Eadie et al. 1975); however, the phenomena are so complex and sporadic that results obtained from the fitting of idealized theories to the observations are likely to be illusory.

4. Accretion Disks and Coronae

The most detailed evidence for an accretion disk in a binary X-ray system comes from observations of the 35^d cycle of Her X-1, in which the X-ray intensity drops by a factor ~15 during the ~23^d low phase (Giacconi et al. 1973). In addition, Her X-1 shows sudden dips in intensity preceding the 1.7d eclipses, lasting ~1-2 hours, the appearances of which are locked in phase to the 35^d cycle. Many details of the 35^d cycle can be interpreted as occultations of the pulsating source by a precessing, twisted accretion disk (Petterson 1977; Crosa and Boynton 1980), and strong support for the model comes from analysis of optical photometry of the HZ Her (Gerend and Boynton 1976) and from the appearance of a brief high state near the middle of the low part of the 35^d cycle (Jones and Forman 1976).

The dips are clearly photoelectric absorption events, with soft X-ray cutoffs in their spectra implying a column density $N_H \sim 10^{23}$ cm^{-2} of intervening gas (Becker et al. 1977; Parmar et al. 1980). They are interpreted as obscuration by a thickening of the outer disk resulting from the impact of the mass transfer stream from HZ Her. In contrast, the spectrum of Her X-1 during the low phase of the 35^d cycle is similar to that of the high phase (Becker et al. 1977), even including the soft X-ray excess (Fritz et al. 1976). The absence of a soft X-ray cutoff during the low phase suggests that the disk partially eclipses an extended source, which may be a highly ionized corona with $\tau_o \sim 0.1$ and $T \gtrsim 10^8$ K. The equivalent width of the 6.4 keV iron line increases by a factor ~2 during the low phase (Pravdo et al. 1978), implying that the iron line is formed in the extended source. Similar transitions, dips, and persistent emission during low states have been seen in Cen X-3 (Tuohy and Cruise 1975; Pounds et al. 1975; Schreier et al. 1976).

The most compelling evidence for an extended accretion disk corona comes from observations of the 5.57^h binary system 4U 1822-37, which has a hard spectrum but does not pulse (White et al. 1981). The X-ray intensity varies by a factor ~1.5 with a roughly sinusoidal modulation. In addition, a sharp dip by ~50% in the X-ray intensity lasting ~30 m occurs about 1 hr after the minimum of the smooth modulation. The source has a V = 16 blue optical counterpart that varies in phase with the X-ray source by ~1 mag with no significiant color change and a light curve very similar to that of the X-rays (Mason et al. 1980). At a distance D > 0.6 kpc, the source has a 2-20 keV X-ray luminosity $L_X \approx 1.2 \times 10^{35}$ ergs s^{-1} $(D/1\ kpc)^2$.

The X-ray spectrum of 4U 1822-37 exhibits features characteristic of the pulsing sources. The continuum can be represented roughly by a power law with $\alpha \sim 0.1$ that breaks sharply at 17 keV, upon which is superposed a very broad (4 keV FWHM) 6.7 keV iron emission line with an equivalent width ~1.1 keV. The spectrum has a soft X-ray cutoff indicating absorbing matter with $N_H \sim 2 \times 10^{21}$ cm^{-2}. Remarkably, this cutoff does not vary with the 5.57^h modulation or during the dip, although the spectrum becomes slightly softer at minimum intensity and during the dip.

The absence of spectral changes during the dip rules out photoabsorption by gas with $\tau_o \gtrsim 1$, and clearly indicates a partial eclipse of an extended ($R \sim 0.2\ R_\odot$) accretion disk corona by the companion star. The similarity of the optical light curve to the X-ray light curve and the absence of periodic color changes indicate that the optical source is the accretion disk and corona rather than the companion star, which is likely a red dwarf. White and Holt (1982) suggest that the smooth 5.57^h modulation of 4U 1822-37 is caused by partial occultation of the corona by the outer part of an accretion disk, whose thickness is comparable to R and varies azimuthally. The variation, which is

locked to the binary orbit, may result from the impact of a stream of gas on the accretion disk.

White et al. (1981), White and Holt (1982), and Fabian et al. (1982) have discussed possible models for the accretion disk corona of 4U 1822-37. The spectral break at ~17 keV and the width of the iron line can be attributed to Comptonization in a corona with $\tau_0 \sim 5$. The absence of other strong atomic features in the X-ray spectrum indicates that the gas is highly ionized, and this requires a high X-ray luminosity, $L_x \sim 10^{37}$ ergs s^{-1}, hence a distance ~10 kpc. With a temperature $\sim 10^8$ K, the maximum coronal radius is limited by the gravitational attraction of the neutron star to $R \lesssim 0.3\ R_\odot$, so that the escaping material must be replenished (e.g. by evaporative mass loss from the accretion disk). The central source, which we believe to be an accreting neutron star, may be a pulsator with period $\lesssim 2^s$; if so, the pulsations would be washed out as they diffuse through the corona.

4U 1822-37 is not unique. The source 4U 2129 + 47 has a power law X-ray spectrum with $\alpha \approx 0.9$, a 5.2^h modulation, and a partial eclipse all quite similar to those of 4U1822-37 (White and Holt 1982; McClintock et al. 1982). The same kind of model can also explain the approximately sinusoidal 4.8^h modulation of Cyg X-3 (Parsignault et al. 1977; Elsner et al. 1980b), where the lack of a partial eclipse can be attributed to a lower inclination. Its 2-20 keV spectrum (Becker et al. 1978b; Blissett et al. 1981; White and Holt 1982), which is very similar to that of 4U 1822-37, favors an optically thick corona over a model proposed by Milgrom (1976) for the 4.8^h modulation of Cyg X-3, in which a close ($a \sim 10^{11}$ cm) binary system is surrounded by a thick ($\tau_0 \gtrsim 1$) shell of radius $R \gtrsim 10\ a$; this is because the strong photoelectric absorption features <5 keV and ~8-10 keV implied by Milgrom's model are not observed.

5. Galactic Bulge Sources

In contrast to the pulsating X-ray binaries, most of the persistent sources which do not pulse, such as Sco X-1 (Miyamoto and Matsuoka 1977; Lamb and Sanford 1979; Coe et al. 1980; Johnson et al. 1980), Cyg X-2 (Ulmer et al. 1974), and the galactic bulge sources (Jones 1977; Markert et al. 1977; Ostriker 1977; Lamb and Sanford 1979) appear to have soft bremsstrahlung spectra with 3 keV $\lesssim$ kT $\lesssim$ 8 keV. Because of their high X-ray luminosity, i.e. $10^{36} < L_x < 10^{38}$ ergs s^{-1}, one supposes that they are neutron star binaries with low mass ($\lesssim 0.5\ M_\odot$) companions like the 7.7s X-ray pulsar 4U 1626-67 (Joss and Rappaport 1979). If so, explanations are required for the lack of observed orbital and pulsation periods and for the soft spectra. One explanation for the lack of eclipses (Milgrom 1978) is that they have accretion disks thicker than the companion star, so that the X-ray source is always obscured by the disk if its orbital inclination permits an eclipse. The lack of pulsations might be understood in terms of decay of neutron star magnetic fields in these old Pop II systems (but then 4U 1626-67 would be a counterexample). An alternative explanation (White and Holt 1982) is that some of these systems may be extreme versions of Cyg X-3 and 4U 1822-37, with accretion disk coronae much larger than the companion star. The softer X-ray spectra and the absence of pulsations may be due to Compton scattering in the corona. If this model is correct, it may be fruitful to search for periodic partial occultations of small amplitude in these systems.

6. X-Ray Bursters

There are about 30 known X-ray burst sources, characterized by irregular sudden bursts of X-rays with luminosities reaching $L_x \sim 10^{39}$ ergs s^{-1} and duration ~10-1000 s (Lewin and Joss 1981; Inoue et al. 1981). The X-ray burst spectra can be characterized by blackbodies with temperatures kT ~ 1-3 keV

that are related to the X-ray luminosity by $kT \sim L_X^{1/4}$, with a constant of proportionality that is roughly independent of time as the burst evolves and roughly the same for all sources. This relation may be interpreted as the result of blackbody radiation from the entire surface area of a neutron star of radius R ~ 7-10 km. The maximum spectral temperature of the burst is approximately equal to the blackbody temperature of a neutron star radiating at the Eddington limit: $T_E = [GM_* m_H c/(R^2 \sigma_T \sigma_S)]^{1/4}$. The bursts are believed to result from thermonuclear explosions on the surfaces of accreting neutron stars. Since the explosion seems to cover the entire neutron surface and no pulsations are observed, the neutron star magnetic fields are believed to be weak.

One exception, the so-called "Rapid Burster" (Lewin and Joss 1981), exhibits rapidly repeating bursts with luminosities that correlate with the times since the previous bursts; these bursts are believed to be associated with magnetospheric regulation of the accretion flow to the stellar surface.

D. Stellar Mass Black Holes

Two binary X-ray sources have been identified as likely candidates for black holes: Cygnus X-1 and Circinus X-1. They are unique among the compact binary systems in having rapid (<1s) aperiodic time variability of large amplitude (Rothschild et al. 1977; Toor 1977; Weisskopf and Sutherland 1980) and hard X-ray spectra extending to $\gtrsim$100 keV. The 5.6^d binary Cyg X-1 is the best case, with a probable compact object mass ~10 $M_\odot$ exceeding the limit for a neutron star (Bahcall 1978). The mass of Cir X-1 is unknown; it is suspected to be a black hole because its X-ray variability resembles that of Cyg X-1.

The spectrum of Cyg X-1 has two distinct states. Most of the time it is in its low state with a spectrum that follows a power law ($\alpha \approx 0.6$) for $2 < E < 100$ keV and drops off smoothly for $E > 100$ keV (Sunyaev and Trümper 1979;

Nolan et al. 1981), giving a luminosity $L_x \sim 4 \times 10^{37}$ ergs s^{-1} $(D/2.5 \text{ kpc})^2$. Occasionally ($\lesssim$10%), it enters a high state, in which its spectrum becomes much brighter and steeper ($\alpha \sim 2.1$) for $E < 10$ keV, but remains almost unchanged for $E \gtrsim 10$ keV (Chiappetti et al. 1981; Page et al. 1982).

A simple optically thick accretion disk model (Pringle 1981) for Cyg X-1 would have a maximum photon energy $kT_{BB} \sim 3$ keV, far too low to account for the observations. The favored theoretical model is one in which the observed spectrum is produced by Comptonization of soft photons as they diffuse through a region of high temperature electrons (Shapiro et al. 1976; Liang and Price 1977; Liang 1980). Indeed, the observed spectrum fits the theoretical spectrum fairly well if the hot region has $kT_e \sim 30$ keV and $\tau_o \sim 4$ (Sunyaev and Trümper 1979), although an excess of photons with $E \gtrsim 300$ keV suggests a component of hotter electrons (Mandrou et al. 1978; Nolan et al. 1981).

The origins of the high temperature electrons and of the soft photons are uncertain. When the source luminosity $L \gtrsim 0.02\ L_E$, the inner portion of a "standard" (Shakura and Sunyaev 1973) disk becomes unstable. A possible model for the inner disk is a "two-temperature" disk (Shapiro et al. 1976) that is optically thin and geometrically thick, supported by the thermal pressure of very hot ($kT_i \sim 60$ MeV) ions. The electrons in this inner disk should have a temperature $kT_e \sim 30$-100 keV that is controlled by a balance between Coulomb heating by the hot ions and cooling by Comptonization of the soft photons. The soft photons may come from the cool outer portions of the disk. Alternatively, the Comptonization might occur above a cool disk, in a corona that is heated by some kind of instability, possibly magnetic. Particularly useful discriminators might be measurements of the correlations between time variations of the intensities at different spectral energies (Priedhorsky et al. 1979; Page et al. 1982; Guilbert and Fabian 1982).

Cir X-1 has a 16.6^d period and a massive (>30 $M_\odot$) OB companion star (Whelan et al. 1977). At a distance ~10 kpc, its maximum X-ray luminosity is $\sim 10^{38}$ ergs s^{-1}. Unlike Cyg X-1, Cir X-1 has a steep spectrum for E > 10 keV (Coe et al. 1976; Nolan 1982). The soft X-ray spectrum is highly variable, with a cutoff ranging from ~2 keV to ~10 keV, indicating photoabsorption by gas with column density ranging from $\sim 10^{22}$ cm^{-2} to $\gtrsim 10^{24}$ cm^{-2}. This variability may result from an eccentric (e ~ 0.8) orbit in a very dense stellar wind (Murdin et al. 1980).

E. Active Galactic Nuclei

Our best guess at the energy source for the X-radiation from active galactic nuclei is that it accrues from the gravitational energy liberated at the infall of matter to a central black hole of mass $\gtrsim 10^6$ $M_\odot$. The variety of possible X-ray production and transfer mechanisms is large (e.g. Rees 1980), but some consistent patterns are beginning to emerge. The spectra of all the Sy I nuclei measurable over a dynamic range >10 with HEAO-1, for example, are nearly identical. All are either fit better (or at least no worse) by power laws than by bremsstrahlung continua, with best-fit indices of $\alpha \approx 0.7 \pm 0.1$ (Mushotzky et al 1980, Holt 1981). No steepening at higher energies is evident out to ~40 keV.

There is clearly a reservoir of lower energy photons in AGN that are available for Comptonization. Continuum emission longward of Ly_α is observed, and that shortward is directly responsible for the stimulation of the characteristic broad line emission of Seyferts and quasars (e.g. Davidson and Netzer 1979). If we hypothesize that the observed $\alpha = 0.7$ power law spectrum of these sources is the result of Comptonization by a sub-relativistic ($T \lesssim 10^9$ K) thermal plasma, we may infer from §III.A.3 that $\tau_o \lesssim 3$.

The relatively weak X-ray signals from all but the very closest AGN (typically, $\lesssim 10^{-11}$ ergs cm^{-2} s^{-1}, or $\lesssim 10^{-3}$ that of the Crab nebula), compromise the potential spectroscopic discriminators we need to distinguish Comptonized power law spectra from those produced by nonthermal processes. The present sensitivity does not allow (for a fair sample of AGN) the detection of either low-equivalent-width features in narrow bandwidth ranges, or spectral bends or breaks over broader bandwidth ranges. We return to this problem for AGN (and potential tests for the origin of the observed power law spectra) in §IV.C.

Even if the primary production mechanism is unknown, the X-ray spectra of AGN provide information about the distribution of gas around the central sources. In Sy I's the observed X-ray absorption is presumed to arise in relatively cold "clouds" exterior to the source (cf Davidson and Netzer 1979). If the individual clouds are smaller than the source, and if the average number of clouds along the line of sight is of order unity, we can (in principle) determine several independent geometrical parameters from the spectrum alone. These include the fraction of the source covered by the clouds (from the absorption) and even a measure of the spherical symmetry of the cloud cover (from the ratio of Fe-K absorbed along the line of sight to that measured in reemission). The most sensitive measures of these parameters should occur in sources having a covering factor of ~0.9, since the effects of the partial cover will be most easily interpreted for this situation. Holt et al. (1980) have found that NGC 4151 satisfies this ~90% condition, and have speculated that quasars and higher luminosity Seyferts are less covered (and lower luminosity Seyferts are more covered) than NGC 4151; and lower luminosity Seyferts are more covered; such a situation is indicated from optical measurements and expected if the average distance to the clouds is regulated by the radiation from the central source. New measurements of high (Holt 1981)

and low (Mushotzky et al. 1981b) luminosity Seyferts from the Einstein SSS are consistent with this general picture.

IV. NON-THERMAL SOURCES

A. Physical Processes

The very high radio brightness temperatures and the radio and optical polarization seen in some AGN and the Crab Nebula clearly indicate regions of ordered magnetic field containing a population of relativistic electrons with Lorentz factors $\gamma \gtrsim 10^3$ to 10^6 (Burbidge et al. 1974; Shklovsky 1968). Such nonthermal electrons can produce high energy radiation by bremsstrahlung, synchroton radiation, or inverse Compton radiation. Nonthermal bremsstrahlung, the traditional way by which X-rays are produced on earth, is unlikely to be important in most astrophysical contexts, because the efficiency for production of X-rays by fast electrons is small ($\sim 10^{-4}$) compared to their Coulomb energy loss in the background plasma. In contrast, relativistic electrons will produce synchroton and inverse Compton radiation with efficiency approaching unity if $(U_B+U_R)\gamma^2/nm_ec^2 \gtrsim 10$, where $U_B + U_R$ is the energy density in the magnetic and radiation fields, and n is the number density of ambient particles.

Synchrotron and inverse Compton radiation are discussed thoroughly by Rybicki and Lightman (1979). A relativistic electron moving through a magnetic field with component $B_\perp(G)$ perpendicular to the electron velocity will radiate most of its power in a continuum of harmonics $\sim\gamma^3$ of the gyrofrequency energy, $E_B = 1.2 \times 10^{-11} B_\perp \gamma^{-1}$ keV. Note that ultrarelativistic ($\gamma \gtrsim 10^6$) electrons are required to produce X-rays by synchrotron radiation in most astrophysical sources, where B < 1 G (except some neutron stars and white dwarfs -- cf. §V). Inverse Compton radiation, in which a low-energy (E_o) photon is scattered by a

relativistic electron, produces photons with typical energies $E \sim 4/3\ E_0\gamma^2$. Thus $\gamma \sim 50$ is sufficient to upscatter optical photons to 1 keV, for example. Synchrotron radiation and inverse Compton radiation are formally very similar. Both produce power law spectra with spectral index $\alpha = (\Gamma-1)/2$ if the relativistic electron number spectrum is a power law, $dn_e/d\gamma \propto \gamma^{-\Gamma}$.

The electron radiation lifetime is given by $t_{rad}(\gamma) \sim m_e c^2/[\gamma\sigma_T c(U_B+U_R)]$. Radiative decay of relativistic electrons can cause slope changes in nonthermal spectra that may provide important information about the source (e.g., Ramaty 1974). For example, a power law electron spectrum injected at time $t = 0$ will develop a sharp cutoff at $\gamma_{cr}(t)$ such that $t_{rad}(\gamma_{cr}) = t$. However, if the electron injection is continuous, there will be only a unit increase in Γ for $\gamma > \gamma_{cr}(t)$, where t is the age or leakage time out of the source, causing a half-unit increase in α at $E(\gamma_{cr})$. Spectral flattening with increasing energy may result from higher order scattering, i.e., Compton scattering of synchrotron photons by the electrons responsible for their primary production.

B. Crab Nebula

Rather than having the thermal X-ray spectrum of most other supernova remnants (§IID), the Crab nebula spectrum is a featureless power law with $\alpha = 1.0$ (i.e., equal power in each decade of energy) to $\gtrsim$500 keV, giving a total nebular luminosity $>10^{38}$ ergs s^{-1}. The long-standing enigma of the origin of this luminosity was resolved by the discovery of the pulsar NP 0531+21, and the subsequent understanding that the power derives from the electromagnetic braking of the rapidly rotating neutron star (e.g., Manchester and Taylor 1977).

The pulsar represents <10% of the total nebular X-ray luminosity below 10 keV, but contributes an increasing fraction at higher energies (i.e., it appears to have a power law energy spectrum somewhat flatter than that of

the nebula, e.g. Strickman et al. 1979; Pravdo and Serlemitsos 1981). The electrodynamics of the Crab pulsar are not well understood, but it is clear that the pulsar X-ray emission is highly anisotropic and nonthermal.

The nebular situation is somewhat simpler to model, at least in a general way. The emission must be synchrotron in origin, because the measured X-ray polarization, at a level of 20% (Weisskopf et al. 1978), is parallel to the optical polarization, which has long been understood to be a synchrotron source. Equipartition estimates of the nebular magnetic field $\sim 3 \times 10^{-4}$ G imply a radiation lifetime $t_{rad} \lesssim 10$ y for the relativistic ($\gamma \sim 10^7$) electrons responsible for the 1 keV X-ray emission. The electrons responsible for the higher energy X-rays have even shorter lifetimes, perhaps less than the light travel time to the pulsar, requiring an in situ acceleration mechanism (Melrose 1969) possibly related to the moving "wisps" observed in the nebular optical continuum (Scargle 1969). The mechanisms for the transport of the pulsar power through the nebula and for the acceleration of the electrons are not well understood; observations of the morphology change of the nebula with increasing X-ray energy (e.g., Pelling et al. 1982) may provide vital clues.

The soft X-ray morphology of the Crab is very different from that of the blast-wave SNR's like Cas A or Tycho. In X-rays, as in radio, the emission is diffuse over the nebular volume instead of being limb-brightened. The Crab Nebula blast wave probably propagated into an ISM much less dense than that surrounding the progenitors of Cas A or Tycho, so that the snowplow effect will never manifest itself in a strong shell source in the Crab. No evidence for line emission has been obtained with Einstein spectrometers. The Vela pulsar appears to be a somewhat older version of the Crab. SN 1006 resembles the Crab in having a filled morphology and a continuum X-ray spectrum with no line emission (Becker et al. 1980c), but no pulsar has yet been found.

C. Active Galactic Nuclei

Direct synchrotron emission is unlikely to account for the X-ray emission from most AGN. In contrast to the Crab nebula, where a legacy of kinetic energy is used to power the X-ray source, fresh fuel in the form of mass flow $\dot{M} \sim 2 \times 10^{-3}\ \eta^{-1}\ L_{44}\ M_{\odot}\ yr^{-1}$ is required. This mass flow, and the necessity of a source dimension <one light day in some AGN (see below), make it likely that the characteristic time scale for Compton production of X-rays from available lower energy photons would be much shorter than that for direct synchrotron radiation. For example, in the Crab nebula high-energy γ-rays must be produced from the upscattering of synchrotron photons by the parent electrons (Gould 1965). Self-Synchrotron-Compton (SSC) models for AGN (Jones et al. 1974) suggest that the radio emission originates from ultrarelativistic electrons, as it does in radio galaxies, but that the X-rays result from first-order Compton scattering of the radio photons. For typical radio spectra, with index $\alpha \sim 0.5$, the resultant X-ray flux can be related to the field B and the geometry through the frequency ν_m at which synchrotron self-absorption is manifested in the radio band, i.e. $F_x \propto \nu_m^{-6.5} F_m^5 \theta^{-8}$ (where $B \propto \nu_m^5 \theta^4 F_m^{-2}$, F_m is the flux thath would be measured at ν_m if there were no self-absorption, and θ is the angular extent of the source on the sky). Clearly, the dependences on ν_m and θ are so strong that F_x can easily be fit with a spectrum similar in slope to the unscattered radio spectrum.

The fundamental question of whether the X-rays from AGN are produced by non-thermal ultrarelativistic electrons or by Comptonization by hot thermal electrons may be resolved by observations of their hard X-ray and gamma-ray spectra. The sudden onset of rapid pair production processes makes it very unlikely that a thermal plasma will have an electron temperature $kT_e \gtrsim 1$ MeV (e.g., Rees 1982; Lightman 1982). Therefore, X-rays produced by thermal Comptonization should

have a break in their spectrum in the range 100 keV $\lesssim E \lesssim$ 10 MeV, while X-ray spectra produced by relativistic electrons may extrapolate smoothly across this range. A few extragalactic sources, including NGC 4151, 3C273, and Cen A have been detected at energies $\gtrsim$1 MeV (Dean and Ramsden 1981), but their spectra have not been measured accurately enough to determine whether such a break exists.

With synchrotron, SSC and Comptonized models yielding spectra that are indistinguishable at the current sensitivity level, other information must be utilized to further probe the nature of the emission process. The most useful constraints for determining the origins of apparently non-thermal spectral forms are probably provided by measurements of temporal variability. Traditionally, the minimum variability timescale has been used to define a minimum source dimension, i.e. $R \lesssim c\Delta t$. For a source through which the photons must diffuse before emerging, the observed timescale for variability will exceed the true minimum source dimension by the factor $(1 + \tau_o)$. Cavallo and Rees (1978) have derived a relation between the matter density n interior to R and the minimum efficiency ε with which it can be converted to radiation implied by the timescale for variability in the luminosity L, i.e. $L\Delta t \approx \varepsilon(\frac{4}{3}\pi R^3 n)\, m_H c^2$. Unless there is relativistic outflow in the source, the above temporal considerations are model-independent (as are a variety of other potential indicators, e.g. Cavaliere and Morrison 1980).

The only temporal variations reliably observed in Seyfert galaxies have been from NGC 4151 and NGC 6814. The minimum timescale for variability in the former is approximately one day (Mushotzky et al. 1978b), which limits the efficiency for radiation production to <1%. NGC 6814, however, with measurable variability on timescales of ~100 s, must have $\varepsilon \approx$ 10% (Tennant et al. 1981). This fast time variability also constrains any SSC model for

NGC 6814 to require continuous acceleration or injection, as the timescale for Compton scattering energy loss is much smaller than the $R = c\Delta t$ size (note that the energy loss timescale is proportional to the square of the variability timescale, so that this conclusion does not apply to NGC 4151). However, thermal Comptonization models (§III) encounter no such problems and will work for both of these sources and most quasars.

BL Lac sources differ considerably from Sy I galaxies in two important qualitative respects: they are more variable, and they are powerful radio emitters. BL Lacs are also the only AGNs known to exhibit pronounced spectral variability in X-rays. The five BL Lacs for which spectra are available from HEAO-1 and HEAO-2 demonstrate very soft ($\alpha > 2$) spectra near ~1 keV, and a highly variable flat ($\alpha \sim 0$) high energy extension (Holt 1981; Worrall et al. 1981). These data are consistent with SSC models, although with relativistic beaming required (Urry and Mushotzky 1982), where the flat high energy extension represents the first-order Compton-scattered component of a synchrotron spectrum that may extend out to the steep X-ray component.

Quasars may represent a less uniform set than do either Sy I or BL Lac sources, but much of the evidence is circumstantial. Most quasars are barely distinguishable from Sy I galaxies, and are generally labeled the latter if evidence for spiral structure in the galaxy is observed (e.g. Wilson and Penston 1979); like Sy I's, most quasars are relatively radio quiet. There are only two quasars for which X-ray continuum measurements over a dynamic range $\gtrsim 10$ have been measured: 3C 273 (Worrall et al. 1979), and QSO 0241 (Worrall et al. 1980). The $\alpha = 1.0$ spectrum of the latter, which is a radio quiet quasar, is only marginally steeper than the $\alpha = 0.7$ average for Sy Is. The $\alpha = 0.4$ spectrum of 3C 273, a radio loud quasar, has a statistical precision identifying it as distinctly flatter than the Sy I average. Zamorani et al.

(1981), over a smaller dynamic range near ~1 keV, report that an $\alpha = 0.4$ spectrum may be typical of radio loud quasars. It is likely that the X-ray production and transport mechanisms in the radio quiet quasars are similar to those in Sy Is. It may be that the radio loud quasars have more in common with BL Lacs, in which case their hard spectra may represent first-order Compton scattering of IR photons by relativistic electrons.

D. The Diffuse X-Ray Background

The isotropy of the diffuse background (XRB) demands either a truly diffuse production mechanism or an origin in discrete sources at earlier epochs. Cowsik and Kobetich (1972) noted that the available data could be reasonably well-fit to the bremsstrahlung spectrum of a plasma at $T \sim 30$ keV. Field and Perrenod (1977) examined the constraints on a hot intergalactic plasma that might be responsible for the XRB, noting the difficulties associated with a truly diffuse model even if clumping is taken into account. Setti and Woltjer (1979) argued that a conventional evolutionary scenario, normalized at the three quasars detectable in X-rays with pre-Einstein sensitivity, would have no trouble exceeding the measured XRB. Measurements from Einstein of deep surveys (Giacconi et al. 1979b) and preselected quasars (Tananbaum et al. 1979) seemed to confirm this convergence to an XRB dominated by the contribution from quasars (Giacconi 1980).

The XRB spectrum is now well-measured in the 3-50 keV band, where it has its peak energy density, and is remarkably well-fit by a 40 keV bremsstrahlung spectrum (Marshall et al. 1980). These spectral data are not easily reconciled with quasars, or with any other extragalactic sources observed locally. Clusters of galaxies are too cool (and too sparse) to be major contributors. BL Lacs are also too sparse, as they do not exhibit the evolutionary enhancement of quasars; furthermore, it is only the variable high energy tails of their two-

component spectra that might contribute significantly to the energy density of the XRB, rather than the steep components which are much more easily detectable at ~1 keV.

Seyferts, with $\alpha \approx 0.7$, have spectra that, while considerably harder than the low energy BL Lac components, are still unacceptably soft $\lesssim$20 keV, where the 40 keV bremsstrahlung spectrum can be approximated by $\alpha \approx 0.4$. Interestingly, the measured luminosity distribution of local Seyferts (Piccinotti et al. 1982) can match the observed low energy gamma-ray background (Kinzer et al. 1978) if these spectra are maintained out to $\gtrsim$100 keV.

If we presume that the radio-quiet quasars (>90% of all quasars) are spectrally similar to Sy I's, the difficulty in producing the XRB from quasars becomes acute. The consistency of the 3C 273 spectrum with $\alpha = 0.4$ suggests that the radio loud quasars might be important contributors (especially since the ~1 keV X-ray luminosity of radio-loud quasars apparently correlates with radio luminosity, Zamorani et al. 1981), but the positive detection by Cos-B of gamma rays from 3C 273 led Setti and Woltjer (1979) to conclude that 3C 273-like quasars cannot contribute more than ~5% of the XRB without overproducing the gamma-ray background.

Subtracting the "known" contributors, i.e. clusters and Seyferts, the remainder of the XRB cannot be easily fit with a distribution of power law sources unless they have breaks allowing them to mock an apparent bremsstrahlung spectrum (Cavaliere et al. 1979; DeZotti et al. 1982). Based on radio/optical/ X-ray correlations, Cavaliere et al. (1981) and Kembhavi and Fabian (1982) have concluded that quasars cannot dominate the XRB at ~10 keV and >2 keV, respectively. At lower energies, they might easily dominate the XRB, but without contributing substantially to the >10 keV energy density (Holt 1980c).

If quasars cannot explain the XRB, what can? A diffuse intergalactic thermal component can explain the spectrum, but the theoretical implications may be too imposing (Field and Perrenod 1977). The problem would be resolved if a now extinct class of emitters with apparently thermal spectra at the appropriate temperature exist at an earlier epoch. Bookbinder et al. (1980) have suggested that "ordinary" protogalaxies at $z > 1$, rich in supernovae and binary X-ray sources in young OB associations, might well give rise to galactic winds at temperatures that would mimic the XRB. Boldt and Leiter (1981) have proposed that the protogalaxies of less ordinary types [i.e. those (at $z \approx 4$) that mature into AGNs] might be responsible. We are unaware of any data that can unambiguously resolve this puzzle.

V. EFFECTS OF STRONG MAGNETIC FIELDS

A. Physical Processes

Magnetic fields in the range of 10^6-10^8 G on the surfaces of white dwarf stars have been inferred from circular polarization and Zeeman splitting of their optical spectra (Angel 1978), and fields in the range of 10^{11}-10^{13} G on the surfaces of neutron stars have been inferred from the slowing down of radio pulsars (Manchester and Taylor 1977), from the spin-up of pulsating X-ray sources (Ghosh and Lamb 1979), and from X-ray spectral features interpreted as cyclotron resonance (Trümper et al. 1978). Such magnetic fields can drastically modify the hydrodynamics of the accretion flow and the spectral formation mechanism, and they are essential to the mechanism for X-ray pulsations in accreting compact objects.

By equating the ram pressure of spherically symmetric accretion to the magnetic stress of a dipole field, we may estimate a critical surface magnetic

field, B_o, of a compact object (radius R), which is sufficient to affect the dynamics of the accretion flow: $B_{cr} \approx (5 \times 10^7\ G) L_{37}^{1/2} (M/M_\odot)^{-1/4} R_6^{-3/4}$. The radius r_A (the "Alfven radius") where the accretion flow is affected is given by $r_A/R \approx (B_o/B_{cr})^{4/7}$.

In such fields thermal electrons may radiate very efficiently at the cyclotron resonance, E_B. In accreting magnetic white dwarfs, $kT_e \gg E_B$, and the cyclotron radiation is emitted in many harmonics extending from the infrared to the UV. The emission of cyclotron radiation by a distribution of thermal electrons is energy dependent and highly anisotropic, and involves radiative transfer in optically thick resonance lines (Lamb and Masters 1979; Chanmugam 1980; Petrosian 1981).

In an accreting neutron star the surface magnetic field may be so great that E_B is in the X-ray spectral range and comparable to kT_e. The transverse motion of an electron is quantized with energy level spacing, E_B. This quantized motion has dramatic effects on the interaction of radiation with matter. For example, Compton scattering discriminates between two polarization modes: (1) the extraordinary mode, for which the scattering cross section, $\sigma \sim \sigma_T(E/E_B)^2$ for $E < E_B$ and which has a strong resonance at E_B; and (2) the ordinary mode, which does not have a resonance and is not suppressed at low frequencies, but has a strong angular dependence: $d\sigma/d\Omega \sim \sigma_T \sin^2\theta$ (Ventura 1979).

B. Accreting Magnetic White Dwarf Stars

These systems are characterized at optical wavelengths by strong ($\gtrsim$10%) circular polarization that varies regularly with a period ranging from ~1-3 hours (Angel 1978). The sources are believed to be white dwarfs with surface magnetic fields of $\sim 10^6$-10^8 G that are rotating synchronously with the binary

period and accreting gas from a companion star (Chanmugam and Wagner 1978). The prototype is AM Her, whose X-ray spectrum (Rothschild et al. 1981) may be characterized by three components: a hard (0.5-50 keV) spectrum that may be fit roughly by a bremsstrahlung continuum with kT ≈ 30 keV; an iron emission line at ~7 keV with an equivalent width ~800 eV; and a soft (0.15-0.5 keV) component that may be fit by a blackbody with $kT_s \sim 20$-40 eV (Tuohy et al. 1981). The observed UV continuum (1200-3000 Å) is consistent with the same blackbody source if $kT_s \approx 28$ eV (Raymond et al. 1979), and implies a soft X-ray luminosity $L_s \sim 3 \times 10^{34}$ $(D/100\ pc)^2$ ergs s^{-1}, which exceeds the hard X-ray luminosity, L_H, by a factor ~100.

Other accreting magnetic white dwarf systems that resemble AM Her in their optical and X-ray properties are AN U Ma (Hearn and Marshall 1979) and 2A 0311-227 (Charles and Mason 1979; Griffiths et al. 1979). The latter source has a remarkable modulation of X-ray spectrum with orbital period, in which the soft X-rays are totally eclipsed and the hard X-rays are partially eclipsed when we are looking directly at the accreting magnetic pole (White 1981; Patterson et al. 1981). This phenomenon may be interpreted as photoabsorption of X-rays by a magnetically collimated accretion flow.

Cyclotron emission should play an important role in determining the spectrum of an accreting magnetic white dwarf (Lamb and Masters 1979). In the shocked accretion column the thermal broadening of the harmonics of the cyclotron resonance exceeds the line spacing, and the optical depth in the resonances is so great ($\tau_1 \sim 10^9$ at the fundamental) that the region should be opaque from E_B to a harmonic $\ell^* \approx 10\ \Lambda^{0.05}\ (T_e/10^8\ K)^{0.5}$ such that $\tau_{\ell^*} \approx 1$, where $\Lambda_7 = (4\pi\ Ne/10^7\ B)$, and $N(cm^{-2})$ is the electron column density (Wada et al. 1980). Therefore, the spectrum in the range $E_B < E < E^* = \ell^* E_B$ should be a Rayleigh-Jeans Law, $F_E \propto E^2 T_e$, and the luminosity of the optically

thick cyclotron radiation is given by $L_{cyc} \approx (2\times10^{18}$ ergs $s^{-1})(T_e/10^8$ K$)^{5/2}$ $(B/10^8$ G$)^3$ A, where A (cm^2) is the area of the emitting region. When $L_{cyc} \ll L_{ToT}$ (determined by the accretion rate), optically thin bremsstrahlung should dominate the emissivity of the hot gas; roughly half the luminosity should appear as an exponential spectrum with a cutoff at $kT_e \approx kT_{ff} \sim 60$ keV and the other half as blackbody radiation from the surface as in the unmagnetized accreting white dwarf. But for $L_{ToT}/f \lesssim 10^{39}$ ergs s^{-1} $(B/10^8$ G$)^3$, where f is the fraction of the white dwarf surface area encountered by the accretion flow, the cyclotron luminosity should dominate at the expense of the luminosity and temperature, kT_e, of the hard X-ray spectrum.

With a magnetic field $B_o \approx 1.3\times10^7$ G (Young et al. 1981), AM Her should show a strong Rayleigh-Jeans continuum from $E_B \sim 0.15$ eV to $E^* \sim 3$ eV due to cyclotron radiation, with a brightness temperature $kT_e \sim 20$-60 keV. This mechanism probably accounts for the strongly polarized optical continuum radiation of AM Her. However, it is very puzzling that the ratio L_s (28 eV)/L_H (30 keV) ≈ 100. One possible explanation is that the hot emitting region is largely obscured by the cooler unshocked accretion flow, so that most of the hard X-rays are thermalized and reradiated at a cooler temperature kT_s. Alternatively, the soft X-ray luminosity may be due to steady thermonuclear burning of the accreting gas (Weast et al. 1979; Fabbiano et al. 1981).

C. Accreting Magnetized Neutron Stars

Basko and Sunyaev (1975) showed how anisotropies associated with the radiative transfer in strong magnetic fields might lead to the beaming pattern of pulsating X-ray sources; they also pointed out the possibility of a strong emission line in the X-ray spectrum at E_B. Subsequently, a feature at ~58 keV was detected in the spectrum of Her X-1 (Trümper et al. 1978; Gruber et al.

1980), whose interpretation as a cyclotron resonance implied a neutron star surface magnetic field of $\sim 6 \times 10^{12}$ G, allowing for gravitational redshift. Similar spectral features in the range 20-50 keV may have been detected in the spectra of other pulsating X-ray sources (Pravdo et al. 1979; Wheaton et al. 1979; Rose et al. 1979) and of gamma ray burst sources (Mazets et al. 1981). If these spectral features are indeed due to cyclotron resonance, they provide the first direct measurements of neutron star magnetic fields and offer the exciting possibility of using the spectra of the pulsating X-ray sources to infer the physical conditions and geometry of the emitting regions at the surface of an accreting magnetized neutron star.

The proper modeling of the interrelated problems of the hydrodynamics of the accretion flow, the kinetic theory of the emitting region, and the radiative transfer of the X-rays is far from solved, even for highly idealized source models. Indeed, it is not even known whether the radiation should emerge in a pencil beam or a fan beam, or whether the feature observed in the spectrum of Her X-1 should be interpreted as an emission line at ~58 keV or an absorption line at ~45 keV (Lamb 1977). Despite these difficulties, considerable progress has been made toward developing the theory of radiative transfer in strong magnetic fields and studies of model problems have yielded some valuable insights (Wasserman and Salpeter 1980; Nagel 1981a,b; Mészáros and Bonazzola 1981; Pravdo and Bussard 1981; and references therein). These calculations refer to an idealized model of a uniform isothermal slab of gas, so that the beaming pattern arises entirely from the anisotropy of the cross sections. The cyclotron resonance line is formed much closer to the surface of the emitting region than the continuum. If the region is optically thin in the continuum, the line is likely to appear in emission, but otherwise it is likely to be an absorption line. The formation of the resonance line depends

critically on frequency redistribution; line radiation escapes primarily by diffusing to the wings. Therefore, the width of the line depends on the optical depth of the emitting region. It is essential to keep track of the polarization because mode conversion may play a critical role in the spectral formation. At lower frequencies the extraordinary mode is formed deeper in the atmosphere than the ordinary mode, but at the resonance the opposite is true. Therefore, one would expect the beam shape, hence the pulse profile, to change dramatically with frequency.

These effects may be responsible for the dramatic variations of pulse profile with photon energy that have been observed in a few sources such as A0535+26 (Bradt et al. 1976), 4U 0900-40 (McClintock et al. 1976), and 4U 1626-67 (Pravdo et al. 1979). However, attempts to compare the present theoretical models based on isothermal slabs with the observed pulse spectra are certainly rudimentary. For one thing, the spectrum and angular distribution depend critically on temperature gradients in the emitting region, which in turn depend on the mechanism for deposition of energy by the infalling gas. It is still uncertain whether the infalling particles are stopped in a shock by nuclear collisions, in which case the energy is deposited at a Compton optical depth $\tau_0 \approx 50$ (Basko and Sunyaev 1975), by Coulomb collisions with ions at a Compton optical depth $\tau_0 \sim 1$ (Kirk and Galloway 1981), or without a shock by the pressure of the emergent radiation. Furthermore, the pulse profile will certainly depend on the geometry of the emitting region, and hence on the solution of the hydrodynamic problem. The emitting region may not resemble a slab at all; for example, it may be a hollow funnel (Basko and Sunyaev 1975). The absence of reflection symmetry in the observed pulse profiles implies a lack of azimuthal symmetry in the emitting region, so the geometry is likely to be very complicated.

It appears that the understanding of the emitting regions of the pulsating X-ray sources will require a concerted program of theoretical studies and spectrally resolved observations of pulse profiles. Observations of the polarized spectra of the X-ray pulsations in particular may yield useful clues to the physics of these remarkable sources.

VI. CONCLUSIONS

The development of experiments with higher resolving power for X-ray astronomical spectroscopy will have its most obvious application to optically thin sources (§II). The gas in galaxy clusters is so hot and tenuous that the large fraction of the spectroscopic information available can be obtained from the separation of the ionization states of iron. For this task, relatively modest resolving power ($R = E/\Delta E \sim 100$) is adequate, so that dispersive devices may not be required to extract the essential facts.

For lower temperatures and higher densities, higher resolving power becomes more important. For stellar coronae, where the densities are high enough to assure that we are observing near-equilibrium conditions, we have the full range of temperature and density diagnostics described in §II. For these sources, therefore, $R > 100$ is required to extract an important fraction of the available spectroscopic information. In the case of supernova remnants, the most pressing need is for detailed ionization-hydrodynamic-coupled calculations to explain the present data, since most of the spectroscopic effects already observed are not adequately explained. Spatially resolved spectral observations are required to distinguish between the spectral components from supernova ejecta and interstellar gas, and to address the complex shock geometry that may result from interstellar clouds.

The galactic binary X-ray sources are diverse in nature, including white dwarfs and neutron stars with and without strong magnetic fields, and probably black holes as well. They display a rich variety of temporal and spectral behavior. By virtue of continued observations with several X-ray experiments, patterns have begun to emerge that may enable us to understand the physics of the accretion flow and X-ray emission in these sources and the nature of the different classes of sources. The most revealing kinds of observations may be those of spectral variability on timescales ranging from milliseconds to years. There is a clear need for more intensive and extensive observations of the type that have already been done with proportional counters of modest ($R \sim 7$) spectral resolution, but greater area ($\gtrsim 10^4$ cm^2) is required to achieve the necessary sensitivity. An extended spectral range (to $\gtrsim 50$ keV) will be especially valuable for understanding pulse formation in magnetized neutron stars and in accretion disk coronae around neutron stars and black hole candidates. Soft ($\sim$0.2-1 keV) X-ray spectral capability with $R \gtrsim 10$ will provide vital clues to the nature of accretion disks and the magnetosphere of accreting neutron stars, and to the X-ray emission region of accreting white dwarfs.

The spectral structure at $\sim$6-8 keV due to iron K-fluorescence and absorption can be used to infer ionization, temperature, velocity, and geometry of gas near compact galactic and extragalactic X-ray sources. The observed features are prominent, but the resolving power available up to now ($R \sim 7$) has been adequate only to prove the potential of these features as physical diagnostics. With a resolving power of $R \sim 50$ (feasible even with non-dispersive detectors), spectral observations of iron lines will become a powerful tool for understanding accretion flows onto compact objects. More resolving power can be most useful as a probe of material in the line-of-sight to the continuum source (rather than the continuum source itself), as

evidenced by the present modeling of iron absorption and reemission from cold clouds in NGC 4151.

Both the Comptonized sources of §III and the high energy sources of §IV are characterized primarily by continua, so that high resolution may be less important than extended bandwidth for studying the source spectra directly. Since most of the active galactic nuclei spectra we observe have $\alpha < 1$, it is clear that observations at energies higher than the traditional X-ray band are required in order to constrain their total power output.

The extent to which active galactic nuclei contribute to the diffuse X-ray background will remain an open issue until such time as the sensitivity exists to measure the spectra of a sample of AGN at $z > 1$ at energies $\gtrsim 10$ keV. Anything less restricts us to inconclusive consistency arguments about extrapolated spectra. It is true that any potential diffuse X-ray-emitting hot gas cannot be sufficiently dense to close the Universe by itself, but the present limits on the contribution to the measured X-ray background from a hot intergalactic medium, from quasars, or from a new kind of protogalaxy not presently observed at the current epoch, are not sufficient to firmly establish the origin of the XRB.

The new science of cosmic X-ray spectroscopy has already given us important insights into a very broad range of astronomical phenomena. Technology is advancing rapidly, so that large ($\gtrsim 10$) gains in sensitivity and resolving powers are probable with the next generation of X-ray telescopes. These advances may provide the essential tools for understanding the physical conditions in the exotic and fascinating sources that comprise the X-ray sky.

Acknowledgment

This work was partially supported by a grant from NASA to the University of Colorado.

Literature Cited

Angel, J. R. P. 1978. Ann. Rev. Astron. Astrophys. 16: 487-519

Arnett, W. D. 1979. Ap. J. Lett. 230: L37-40

Bai, T. 1979. Solar Phys. 62: 113-121 (Erratum 64: 417)

Bai, T. 1980. Ap. J. 239: 999-1009

Baity, W. A., et al. 1981. Ap. J. 244: 429-435

Bahcall, J. N. 1978, Ann. Rev. Astron. Astrophys. 16: 241-264

Bahcall, J. N., Sarazin, C. L. 1978, Ap. J. 219: 781-94

Basko, M. M. 1978. Ap. J. 223: 268-281

Basko, M. M. 1980. Astron. Astrophys. 87: 330-338

Basko, M. M., Sunyaev, R. A. 1975. Astron. Astrophys. 42: 311-321

Basko, M. M., Sunyaev, R. A. 1976. MNRAS 175: 395-417

Basko, M. M., Sunyaev, R. A., Titarchuk, L. G. 1974. Astron. Astrophys. 31: 249-263

Becker, R. H., Boldt, E. A., Holt, S. S. Pravdo, S. H., Robinson-Saba, J., Serlemitsos, P. J., Swank, J. H. 1979b. Ap. J. Lett. 227: L21-24

Becker, R. H., Boldt, E. A., Holt, S. S., Pravdo, S. H., Rothschild, R. E., Serlemitsos, P. J., Smith, B. W., Swank, J. H. 1977. Ap. J. 214: 879-884

Becker, R. H., Boldt, E. A., Holt, S. S., Serlemitsos, P. J., White, N. E. 1980a. Ap. J. Lett. 237: L77-79

Becker, R. H., Holt, S. S., Smith, B. W., White, N. E., Boldt, E. A., Mushotzky, R. F., Serlemitsos, P. J. 1979a. Ap. J. Lett. 234: L73-76

Becker, R. H., Holt, S. S., Smith, B. W., White, N. E., Boldt, E. A., Mushotzky, R. F., Serlemitsos, P. J. 1980b. Ap. J. Lett. 235: L5-8

Becker, R. H., Robinson-Saba, J. L., Boldt, E. A., Holt, S. S., Pravdo, S. H., Serlemitsos, P. J., Swank, J. H. 1978b. Ap. J. Lett. 224: L113-117

Becker, R. H., Rothschild, R. E., Boldt, E. A., Holt, S. S., Pravdo, S. H., Serlemitsos, P. J., Swank, J. H. 1978a. Ap. J. 221: 912-916

Becker, R. H., Szymkowiak, A. E., Boldt, E. A., Holt, S. S., Serlemitsos, P. J. 1980c. Ap. J. Lett. 240: L33-35

Blissett, R. J., Mason, K. O., Culhane, J. L. 1981. MNRAS 194:77-84

Boldt, E. A., Leiter, D. 1981. Nature 290: 483-485

Bookbinder, J., Cowie, L. L., Krolik, J. H., Ostriker, J. P., Rees, M. J. 1980. Ap. J. 237: 647-654

Bradt, H., et al. 1976. Ap. J. Lett. 204: L67-71

Bradt, H., McClintock, J. 1982. Ann. Rev. Astron. Astrophysics. Submitted

Buff, J., McCray, R. 1974. Ap. J. Lett. 188: L37-40

Bunner, A. N., Sanders, W. T. 1979. Ap. J. Lett. 228: L19-22

Burbidge, G. R., Jonas, T. W., O'Dell, S. L. 1974. Ap. J. 193: 43-54

Canizares, C. R., Clark, G. W., Markert, T. H., Berg, C., Smedira, M., Bardas, D., Schnopper, H., Kalata, K. 1979. Ap. J. Lett. 234: L33-37

Carlberg, R. G. 1978. Ap. J. 220: 1041-1050

Cassinelli, J. P., Olson, G. L. 1979. Ap. J. 229:304-317

Cassinelli, J. P., Swank, J. K. 1982. To be published

Cassinelli, J. P., Waldron, W. L., Sanders, W. T., Harnden, F. R., Rosner, R., Vaiana, G. S. 1981. Ap. J. 250: 677-686

Cavaliere, A., Danese, L., Dezotti, G., Franceschini, A. 1979. Astron. Astrophys. 79: 169-173

Cavaliere, A., Danese, L., Dezotti, G., Franceschini, A. 1981. Astron. Astrophys. 97: 269-273

Cavaliere, A., Morrison, P. 1980. Ap. J. Lett. 238: 63-66

Cavallo, G., Rees, M. J. 1978. MNRAS 183:359-366

Chanmugam, G. 1980. Ap. J. 241:1122-1130

Chanmugam, G., Wagner, R. L. 1978. Ap. J. 222: 641-646

Charles, P. A., Mason, K. O. 1979. Ap. J. Lett. 232: L25-26

Charles, P. A., Mason, K. O., White, N. E., Culhane, J. L., Sanford, P. W., Moffat, A.F.J. 1978. MNRAS 183: 813-820

Chevalier, R. 1982. Ap. J. In press

Chiappetti, L., Blissett, R. J., Branduardi-Raymont, G., Bell Burnell, S. J., Ives, J. C., Parmer, A. N., Sanford, P. W. 1981. MNRAS 197: 139-150

Coe, M. J., Dennis, B. R., Dolan, J. F., Crannell, C. J., Maurer, G. S., Frost, K. J., Orwig, L. E., Graf, W., Price, K. M. 1980. Ap. J. 237: 148-153

Coe, A. M., Engel, A. R., Quenby, J. J. 1976, Nature. 262: 563-564

Colgate, S. A., McKee, C. 1969. Ap. J. 157: 623-643

Conti, P. S., McCray, R. 1980. Science 208: 9-17

Cordova, F. A., Mason, K. O., Nelson, J. E. 1981. Ap. J. 245: 609-617

Cowie, L. L., Binney, J. 1977. Ap. J. 215: 723-732

Cowley, A. P., Crampton, D., Hutchings, J. P. 1979. Ap. J. 231: 539-550

Cowsik, R., Kobetich, E. J. 1972. Ap. J. 177: 585-593

Crosa, L. Boynton, P. E. 1980. Ap. J. 238: 999-1015

Davidson, L., Netzer, H. 1979. Rev. Mod. Phys. 51: 715-766

Dean, A. J., Ramsden, D. 1981. Phil. Trans. R. Soc. London Ser. A 301: 577-602

DeZotti, G., et al. 1982. Ap. J. 253: 47-52

Dubau, J., Gabriel, R. H., Loulergue, M., Steenman-Clark, L., Volonte, S. 1981. MNRAS 195: 705-720

Eadie, G., Peacock, A., Pounds, K. A., Watson, M., Jackson, J. C., Hunt, R. 1975. MNRAS 172: 35p-39p

Elsner, R. F., Ghosh, P., Darbro, W., Weisskopf, M. C., Sutherland, P. G., Grindlay, J. E. 1980b. Ap. J. 239: 335-344

Elsner, R. F., Ghosh, P., Lamb, F. K. 1980a. Ap. J. Lett. 241: L155-160

Fabbiano, G., Hartmann, L., Raymond, J., Steiner, J., Branduardi-Raymont, G., Matilsky, T. 1981. Ap. J. 243: 911-925

Fabian, A. C., Guilbert, P. W., Ross, R. R. 1982. MNRAS In press

Fabian, A. C. Nulsen, P. E. J. 1977. MNRAS 180: 479-484

Felsteiner, J., Opher, R. 1976. Astron. Astrophys. 46: 189-195

Field, G., Perrenod, S. 1977. Ap. J. 215: 717-722

Fireman, E. L. 1974. Ap. J. 187: 57-60

Forman, W., Jones, C. 1982. Ann. Rev. Astron. Astrophys. 20: In press

Fransson, C., Fabian, A. C. 1980. Astron. Astrophys. 87: 102-108

Fritz, G., Naranan, S., Shulman, S., Yentis, D., Friedman, H., Davidson, A., Henry, R., Snyder, W. 1976. Ap. J. Lett. 207: L29-32

Garmire, G. 1979. HEAO Science Symposium, ed. C. Dailey, W. Johnson, p. 49-81. NASA CP-2113

Gerend, D., Boynton, P. E. 1976. Ap. J. 209:562-573

Ghosh, P., Lamb, F. K. 1979. Ap. J. 234: 296-316

Giacconi, R. 1980. X-Ray Astronomy, ed. R. Giacconi, G. Setti, p. 385-398. Dordrecht: Reidel

Giacconi, R., Gursky, H., Kellogg, E., Levinson, R., Schreier, E., Tananbaum, H. 1973. Ap. J. 184: 227-236

Giacconi, R. et al. 1979a. Ap. J. 230: 540-550

Giacconi, R. et al. 1979b, Ap. J. Lett. 234: L1-7

Giacconi, R., Gursky, H., Paolini, F., Rossi, B. 1962. Phys. Rev. Lett. 9: 439-443

Gould, R. J. 1965. Phys. Rev. Lett. 15: 577-579

Griffiths, R. E., Ward, M. J., Blades, J. C., Wilson, A. S., Chaisson, L., Johnston, M. D. 1979. Ap. J. Lett. 232: L27-31

Gronenschild, E.H.B.M., Mewe, R. 1982. Astron. Astrophys. In press

Gruber, D. E. et al. 1980. Ap. J. Lett. 240: L127-131

Guilbert, P. W. 1981. MNRAS 197: 451-460

Guilbert, P. W., Fabian, A. C. 1982. Nature. In press

Hall, D. S. 1976. Multiple Periodic Variable Stars, pp. 287-348. Dordrecht: Reidel

Hatchett, S., McCray, R. 1977. Ap. J. 211: 552-561

Hearn, D. R., Marshall, F. J. 1979. Ap. J. Lett. 232: L21-23

Heiles, C. 1964. Ap. J. 140: 470-476

Hertz, P., Joss, P. C., Rappaport, S. 1978. Ap. J. 224: 614-624

Holt, S. S. 1980a. X-Ray Astronomy, ed. R. Giacconi, G. Setti, pp. 89-102. Dordrecht: Reidel

Holt, S. S. 1980b. Symposium on Space Astrophysics, ed. S. Hayakawa, pp. 227-240. Tokyo: Univ. of Tokyo

Holt, S. S. 1980c. X-Ray Astronomy, ed. R. Giacconi, G. Setti, pp. 327-337. Dordrecht: Reidel

Holt, S. S. 1981. X-Ray Astronomy from the Einstein Observatory, ed. R. Giacconi, pp. 173-185. Dordrecht: Reidel

Holt, S. S., Mushotzky, R. F., Becker, R. H., Boldt, E. A., Serlemitsos, P. J., Szymkowiak, A. E., White, N. E. 1980. Ap. J. Lett. 241: L13-17

Holt, S. S., White, N. E., Becker, R. H., Boldt, E. A., Mushotzky, R. F., Serlemitsos, P. J., Smith, B. W. 1979. Ap. J. Lett. 234: L65-68

Illarionov, A., Kallman, T., McCray, R., Ross, R. R. 1979. Ap. J. 228: 279-292

Illarionov, A. V., Sunyaev, R. A. 1975. Astron. Astrophys. 39: 185-195

Inoue, H. et al. 1981. Ap. J. Lett. 250: L71-75

Itoh, H. 1977. Publ. Astr. Soc. Japan 29: 813-830

Itoh, H. 1978. Publ. Astr. Soc. Japan 30: 489-498. (Erratum 31: 429)

Itoh, H. 1979. Publ. Astr. Soc. Japan 31: 541-562

Jackson, J. C. 1975. MNRAS 172: 483-492

Johnson, W. N., Kurfess, J. D., Maurer, G. S., Strickman, M. S. 1980. Ap. J. 280: 982-989

Jones, C. 1977, Ap. J. 214: 856-873

Jones, C., Forman, W. 1976, Ap. J. Lett. 209: L131-136

Jones, T. W., O'Dell, S. L., Stein, W. A. 1974. Ap. J. 188: 353-368

Joss, P. C., Rappaport, S. 1979. Astron. Astrophys. 71: 217-220

Kallman, T., McCray, R. 1982. Ap. J. Suppl. In press

Katz, J. I. 1976. Ap. J. 206: 910-916

Kembhavi, A. K., Fabian, A. C. 1982. MNRAS In press

Kinzer, R. L., Johnson, W. N., Kurfess, J. D. 1978. Ap. J. 222: 370-378

Kirk, J. G., Galloway, D. J. 1981. MNRAS 195: 45p-50p

Kompaneets, A. S. 1957. Sov. Phys.-JETP 4:730-737

Krasnobaev, K. V., Sunyaev, R. A. 1977. Sov. Astron. Lett. 3: 64-66

Krolik, J., McKee, C. F., Tarter, C. B. 1981, Ap. J., 249: 422-442

Kwan, J. Y., Krolik, J. 1981. Ap. J. 250: 478-507

Kylafis, N. D., Lamb, D. Q. 1979. Ap. J. Lett. 228: L105-110

Kylafis, N. D., Lamb, D. Q. 1982. Ap. J. Suppl. 48: In press

Kylafis, N. D., Lamb, D. Q., Masters, A. R., Weast, G. J. 1980. Annals New York Acad. Sci. 336: 520-549

Lamb, D. Q., Masters, A. R. 1979. Ap. J. Lett. 234: L117-122

Lamb, F. K. 1977. Annals New York Acad. Sci. 302:482-513

Lamb, P., Sanford, P. W. 1979. M.N.R.A.S. 188: 555-563

Langer, S. 1979. Ap. J. 232: 891-894

Langer, S., Ross, R. R., McCray, R. 1978. Ap. J. 222: 959-966

Lewin, W. H. G., Joss, P. C. 1981. Space Sci. Rev. 28: 3-88

Liang, E. T. P. 1979. Ap. J. Lett. 231: L111-114

Liang, E. T. P. 1980. Nature 283: 642-644

Liang, E. T. P., Price. R. U. 1977. Ap. J. 218: 247-252

Lightman, A. P. 1982. Space Sci. Rev. In press

Lightman, A. P., Lamb, D. Q., Rybicki, G. B. 1981. Ap. J. 248: 738-750

Lightman, A. P., Rybicki, G. B. 1979a. Ap. J. Lett. 229: L15-18

Lightman, A. P., Rybicki, G. B. 1979b. Ap. J. 232: 882-890

Long, K. S., White, R. L. 1980. Ap. J. Lett. 239:L65-68

Manchester, R. N., Taylor, J. H. 1977. Pulsars. San Francisco: Freeman

Mandrou, P., Neil, M., Vedrenne, G., Dupont, A., Hurley, K. 1978. Ap. J. 219: 288-291

Markert, T. H., Canizares, C. R., Clark, G. W., Hearn, R., Li, F. K., Sprott, G. F., Winkler, P. F. 1977. Ap. J. 218: 801-804

Marshall, F. E., Boldt, E. A., Holt, S. S., Miller, R. B., Mushotzky, R. F., Rose, L. A., Rothschild, R. E., Serlemitsos, P. J. 1980. Ap. J. 235: 4-10

Mason, K. O., Middleditch, J., Nelson, J. E., White, N. E., Seitzer, P., Touhy, I. R., Hunt, L. K. 1980. Ap. J. Lett. 242: L109-113

Mason, K. O., Branduardi, G., Sanford, P. 1976. Ap. J. Lett. 203: L29-33

Mathews, W. G., Bregman, J. N. 1978. Ap. J. 224: 308-319

Mazets, E. P., Golonetskii, S. V., Aptekar', R. L., Gur'yan, Yu. A., Il'inskii, V. N. 1981. Nature 290: 378-382

McClintock, J. E., et al. 1976. Ap. J. Lett. 206: L99-102

McClintock, J. E., London, R. A., Bond, H. E., Grauer, A. D. 1982, Ap. J.: In press

McCray, R. 1977. Highlights of Astronomy, ed. E. A. Müller Vol. 4, part I: 155-170 (Dordrecht: Reidel).

McCray, R. 1979. Active Galactic Nuclei, eds. C. Hazard, S. Mitton, pp. 227-239 (Cambridge Univ. Press).

McCray, R. 1982. Galactic X-ray Sources. ed. P. Sanford, pp. - . New York: Wiley

McCray, R., Lamb, F. K. 1976, Ap. J. Lett. 204: L115-118

McCray, R., Shull, J. M., Boynton, P. K., Deeter, J. E., Holt, S. S., White, N. E. 1982. Ap. J. In press

McCray, R., Snow, T. P. 1979. Ann. Rev. Astron. Astrophys. 17: 213-240

McKee, C. F. 1974. Ap. J. 188: 335-339

McKee, C. F., Ostriker, J. P. 1977. Ap. J. 218: 148-169

Melrose, D. B. 1969. Ap. Space Sci. 4: 165-181

Mészáros, P., Bonazzola, S. 1981. Ap. J. 251: 695-712

Milgrom, M. 1976. Astron. Astrophys. 51: 215-218

Milgrom, M. 1978. Astron. Astrophys. 67: L25-28

Miyamoto, S., Matsuoka, M. 1977, Space Sci. Rev. 20: 687-755

Murdin, P., Jauncey, Dl. L., Haynes, R. F., Lerche, I., Nicolson, G. D., Holt, S. S., Kaluzienski, L. J. 1980. Astron. Astrophys. 87: 292-298

Mushotzky, R. F., Boldt, E. A., Holt, S. S., Serlemitsos, P. J. 1981b. Bull. Am. Astron. Soc. 12: 873

Mushotzky, R. F., Holt, S. S., Serlemitsos, P. J. 1978b. Ap. J. Lett. 225: L115-118

Mushotzky, R. F., Holt, S. S., Smith, B. W., Boldt, E. A., Serlemitsos, P. J. 1981a. Ap. J. Lett. 244: L47-51

Mushotzky, R. F., Marshall, F. E., Boldt, E. A., Holt, S. S., Serlemitsos, P. J. 1980. Ap. J. 235: 377-385

Mushotzky, R. F., Serlemitsos, P. J., Smith, B. W., Boldt, E. A., Holt, S. S. 1978a. Ap. J. 225: 21-39

Nagel, W. 1981a. Ap. J. 251: 278-287

Nagel, W. 1981b. Ap. J. 251: 288-296

Nolan, P. L. 1982. Ph.D. Thesis, UCSD

Nolan, P. L., Gruber, D. E., Knight, F. K., Matteson, J. L., Rothschild, R. E., Marshall, F. E., Levine, A. M., Primini, F. A. 1981. Nature 293: 275-277

Ostriker, J. P. 1977. Annals New York Acad. Sci. 302: 229-243

Page, C. G., Bennetts, A. J., Ricketts, M. J. 1982. MNRAS. In press

Pallavicini, R., Golub, L., Rosner, R., Vaiana, G. S., Ayres, T., Linsky, J. L. 1981. Ap. J. 248: 279-290

Parmer, A. N., Sanford, P. W., Fabian, A. C. 1980. MNRAS 192: 311-318

Parsignault, D. R., Grindlay, J., Gursky, H., Tucker, W. 1977. Ap. J. 218: 232-242

Patterson, J., Williams, G., Hiltner, W. A. 1981. Ap. J. 245: 618-623

Payne, D. G. 1980. Ap. J. 237: 951-963

Peacock, A., Andresen, R. D., Leimann, E. A., Long, A. E., Manzo, G., Taylor, B. G. 1980. Nucl. Instr. Meth. 169: 613-625

Pelling, M., et al. 1982. Ap. J. Submitted

Petrosian, V. 1981. Ap. J. 251: 727-738

Petterson, J. R. 1977. Ap. J. 218: 783-791

Piccinotti, G., Mushotzky, R. F., Boldt, E. A., Holt, S. S., Marshall, F. E., Serlemitsos, P. J. Shafer, R. A. 1982. Ap. J. 253: In press

Pounds, K. A., Cooke, B. A., Ricketts, M. J., Turner, M. J., Elvis, M. 1975. MNRAS 172: 473-481

Pozdnyakov, L. A., Sobol, I. M ., Sunyaev, R. A. 1979. Astron. Astrophys. 75: 214-222

Pradhan, A. K., Shull, J. M. 1981. Ap. J. 249: 821-830

Pravdo, S. H. 1979. X-Ray Astronomy, ed. W. Baity, L. Peterson, pp. 169-182. Oxford: Pergamon

Pravdo, S. H., Becker, R. H., Boldt, E. A., Holt, S. S., Serlemitsos, P. J., Swank, J. H. 1977. Ap. J. Lett. 215: L61-64

Pravdo, S. H., Boldt, E. A., Holt, S. S., Rothschild, R. E., Serlemitsos, P. J. 1978. Ap. J. Lett. 225: L53-58

Pravdo, S. H., Bussard, R. W. 1981. Ap. J. Lett. 246: L115-120

Pravdo, S. H., Serlemitsos, P. J. 1981. Ap. J. 246: 484-488

Pravdo, S. H., Smith, B. W. 1979. Ap. J. Lett. 234: L195-198

Pravdo, S. H., White, N. E., Boldt, E. A., Holt, S. S., Serlemitsos, P. J., Swank, J. H. 1979. Ap. J. 231: 912-918

Priedhorsky, W., Garmire, G. P., Rothschild, R. E., Boldt, E., Serlemitsos, P., Holt, S. 1979. Ap. J. 233: 350-363

Pringle, J. E. 1981. Ann. Rev. Astron. Astrophys. 19: 137-162

Pringle, J. E., Savonije, G. J. 1979. MNRAS 187: 777-784

Ramaty, R. 1974. High Energy Particles and Quanta in Astrophysics, ed. F. B. McDonald, C. E. Fichtel, Ch. III, pp. 122-169. Cambridge: MIT Press.

Rappaport, S., Joss, P. C. 1982, Accretion Driven X-ray Sources, ed. W. H. G. Lewin, E. P. J. van den Heuvel. Cambridge Univ. Press.

Raymond, J. C., Black, J. H., Davis, R. J., Dupree, A. K., Gursky, H., Hartmann, L., Matilsky, T. A. 1979. Ap. J. Lett. 230: L95-98

Rees, M. J. 1980. X-Ray Astronomy, ed. R. Giacconi, G. Setti, pp. 339-354. Dordrecht: Reidel

Rees, M. J. 1982. Space Sci. Rev. In press

Robinson, E. L. 1976. Ann. Rev. Astron. Astrophys. 14: 119-142

Rose, L. A., et al. 1979. Ap. J. 231: 919-926

Rosner, R., Tucker, W. H., Vaiana, G. S. 1978. Ap. J. 220: 643-665

Ross, R. R. 1979. Ap. J. 233: 334-343

Ross, R. R., Fabian, A. C. 1980. MNRAS 193: 1p-5p

Ross, R. R., Weaver, R., McCray, R. 1978. Ap. J. 219: 292-299

Rothschild, R. E., Boldt, E. A., Holt, S. S., Serlemitsos, P. J. 1977, Ap. J. 213: 818-826

Rothschild, R. E. et al. 1981. Ap. J. 250: 723-732

Rybicki, G. B., Lightman, A. P. 1979. Radiative Processes in Astrophysics. New York: Wiley

Sandage, A. R. et al. 1966. Ap. J. 146: 316-322

Sarazin, C. L. 1982. Rev. Mod. Phys. In press

Scargle, J. D. 1969. Ap. J. 156: 401-426

Schreier, E. J., Swartz, K., Giacconi, R., Fabbiano, G., Morin, J. 1976. Ap. J. 204: 539-547

Sedov, L. I. 1959. Similarity and Dimensional Methods in Mechanics. New York: Academic

Serlemitsos, P. J., Boldt, E. A., Holt, S. S., Ramaty, R., Brisken, A. F. 1973. Ap. J. Lett. 184: L1-6

Serlemitsos, P. J., Boldt, E. A., Holt, S. S., Rothschild, R. E., Saba, J.L.R. 1975. Ap. J. Lett. 201: L9-13

Setti, G., Woltjer, L. 1979. Astron. Astrophys. 76: L1-2

Shakura, N. I., Sunyaev, R. A. 1973. Astron. Astrophys. 24:337-355

Shapiro, S. L., Lightman, A. P., Eardley, D. M. 1976. Ap. J. 204: 187-199

Shklovsky, I. S. 1968. Supernovae, p. 444. New York: Wiley

Shull, J. M. 1981. Ap. J. Suppl. 46: 27-40

Shull, J. M., Van Steenberg, M. 1982. Ap. J. Suppl. 48: In press

Shull, J. M. 1982. Ap. J. Submitted

Smith, B. W. 1981. X-Ray Astronomy from the Einstein Observatory, ed. R. Giacconi, pp. 51-60. Dordrecht: Reidel

Smith, B. W., Mushotzky, R. F., Serlemitsos, P. J. 1979. Ap. J. 227: 37-51

Spitzer, L. Jr. 1962. Physics of Fully Ionized Gases, 2nd Ed. New York: Wiley

Stewart, G. C., Fabian, A. C. 1981. MNRAS 197: 713-720

Strickman, M. S., Johnson, W. N., Kurfess, J. D. 1979. Ap. J. Lett. 230: L15-19

Sunyaev, R. A., Titarchuk, L. G. 1980. Astron. Astrophys. 86: 121-138

Sunyaev, R. A., Trümper, J. 1979. Nature 279: 506-508

Swank, J. H., Becker, R. H., Boldt, E. A., Holt, S. S., Pravdo, S. H., Rothschild, R. E., Serlemitsos, P. J. 1976. Ap. J. Lett. 209: L57-60

Swank, J. H., White, N. E., Holt, S. S., Becker, R. H. 1981. Ap. J. 246: 208-214

Szymkowiak, A. et al. 1982. Preprint

Tananbaum, H. et al. 1979. Ap. J. Lett. 134: L9-13

Taylor, G. I. 1950. Proc. Roy. Soc. London A 201: 159-174

Tennant, A. F., Mushotzky, R. F., Boldt, E. A., Swank, J. H. 1981. Ap. J. 251: 15-25

Thorne, K. S. 1974. Ap. J. 191: 507-519

Toor, A. 1977. Ap. J. Lett. 215: L57-60

Trümper, J., Pietsch, W., Reppin, C., Voges, W., Staubert, R., Kendziorra, E. 1978. Ap. J. Lett. 219: L105-110

Tucker, W. H. 1970. Astrophys. Space Sci. 11: 12-28

Tuohy, I. R., Cruise, A. M. 1975. MNRAS 171: 33p-39p

Tuohy, I. R., Mason, K. O., Garmire, G. P., Lamb, F. K. 1981. Ap. J. 245: 183-194

Ulmer, M. P., Sammuli, A., Baity, W. A., Wheaton, W. A., Peterson, L. E. 1974. Ap. J. 189: 339-342

Urry, C. M., Mushotzky, R. F. 1982. Ap. J. 253: 38-46

Vaiana, G. S. et al. 1981. Ap. J. 245: 163-182

Ventura, J. 1979. Phys. Rev. D 19: 1684-1695

Wada, T., Shimuzu, A., Suzuki, M., Kato, M., Hoshi, R. 1980. Prog. Theor. Phys. 64: 1986-1994

Walter, F. M., Cash, W., Charles, P. A., Bowyer, C. S. 1980. Ap. J. 236: 212-218

Wasserman, I., Salpeter, E. E. 1980. Ap. J. 241: 1107-1121

Weast, G. J., Durison, R. H., Imamura, J. N., Kylafis, N. D., Lamb, D. Q. 1979. IAU Colloq. No. 53, White Dwarfs and Variable Degenerate Stars, ed. H. M. Van Horn, V. Weidemann, pp. 140-144. Rochester: Univ. of Rochester Press

Weisskopf, M. C., Silver, E. H., Kestenbaum, H. L., Long, K. S., Novick, R. 1978. Ap. J. Lett. 220: L117-121

Weisskopf, M. C., Sutherland, P. G. 1980. Ap. J. 236: 263-269

Wheaton, W. A. et al. 1979. Nature 282: 240-243

Whelan, J. A. J. et al. 1977. M.N.R.A.S. 181: 259-271

White, N. E. 1981. Ap. J. Lett. 244: L85-88

White, N. E., Becker, R. H., Boldt, E. A., Holt, S. S., Serlemitsos, P. J., Swank, J. H. 1981. Ap. J. 247: 994-1002

White, N. E., Holt, S. S. 1982. Ap. J. In press

White, S. D. M., Silk, J. 1980. Ap. J. 241: 864-874

Wilson, A. S., Penston, M. V. 1979. Ap. J. 232: 389-399

Winkler, P. F., Canizares, C. R., Clark, G. W., Markert, T. H., Kalata, K., Schnopper, H. W. 1981. Ap. J. Lett. 246: L27-31

Wolfson, R. 1977. Ap. J. 213: 200-207

Worrall, D. M., Boldt, E. A., Holt, S. S., Serlemitsos, P. J. 1980. Ap. J. 240: 421-428

Worrall, D. M., Boldt, E. A., Holt, S. S., Mushotzky, R. F., Serlemitsos, P. J. 1981. Ap. J. 243: 53-59

Worrall, D. M., Mushotzky, R. F., Boldt, E. A., Holt, S. S., Serlemitsos, P. J. 1979. Ap. J. 232: 683-688

Young, P., Schneider, D. P., Shectman, S. A. 1981. Ap. J. 245: 1043-1053

Zamorani, G. et al. 1981. Ap. J. 245: 357-374

FIGURE CAPTIONS

Fig. 1. Data from an exposure to the Perseus cluster of galaxies with the HEAO-1 A2 proportional counter experiment. The lower points, for which the right-hand scale is appropriate, are the raw data in energy-equivalent pulse-height channels. The higher points, for which the left-hand scale is appropriate, represent the most probable input spectrum consistent with the assumption of an equilibrium thermal spectrum. Note, in particular, that the K_α and K_β Fe emission lines at 6.7 keV and 7.9 keV can be enhanced for display by this model-dependent spectral inversion process.

Fig. 2. A comparison of actual raw data from Tycho's SNR taken with the Einstein SSS and an idealized input spectrum. The data can be fit equally well with Sedov and two-temperature-equilibrium modeling, provided that the abundances of the even-Z elements are free parameters. The idealized input spectrum represents the dominant kT = 0.5 keV component of the two-temperature fit, but with the abundances fixed at solar proportions. The shaded area represents the contribution from Fe-L-blend emission at this temperature, and the blackened area represents the contribution from Si-K-emission components. To facilitate comparison with the raw data (where the abscissa should properly be energy-equivalent pulse-height), the idealized input spectrum is viewed through a column density of 2×10^{21} atoms cm^{-2}. Both the data and model are displayed in 46 eV bins, with the latter smeared to an effective resolution with FWHM ~ bin width (i.e., ~3 times better than the actual SSS FWHM resolution). The K_α and K_β transitions of helium-like ions of Mg, Si, S, Ar, and Ca indicated on the model spectrum are clearly evident

in the data. The two-temperature equilibrium fit of Becker et al. (1980a) to these data has 0.5 keV as the lower temperature, and 4 keV as the higher. Since most of the K-emission arises from the lower temperature plasma, it is clear that marked overabundances in the line-emitting species are required for consistency with the two-temperature model.

Fig. 3. Einstein FPCS spectrum from Puppis A, from Winckler et al. (1981). Note, in particular, the ability of a spectrometer with $E/\Delta E \sim 100$ to separate the resonance (R), intercombination (I) and forbidden (F) components of the Ne IX line blend near 0.9 keV.

Fig. 4. Composite X-ray spectrum of Her X-1 as a function of 1.24 s pulse phase, from McCray et al. (1982). Solid curve: time-averaged spectrum, showing an excess of soft ($E \lesssim 0$ keV) X-rays, a nearly power-law ($\alpha \approx 0.5$) continuum for $2 \lesssim E \lesssim 20$ keV, an iron emission line at $E \approx 7$ keV, a break in the spectrum for $E \gtrsim 20$ keV, and structure at $E \approx 50$ keV that is suggestive of electron cyclotron resonance. Dashed and dotted curves: spectra at the maximum ($\phi = 0.85$) and near the minimum ($\phi = 0.48$), respectively, of the hard X-ray pulse, showing that the peak intensities of the soft X-ray pulse and iron line emission are out of phase with the hard X-ray pulse.

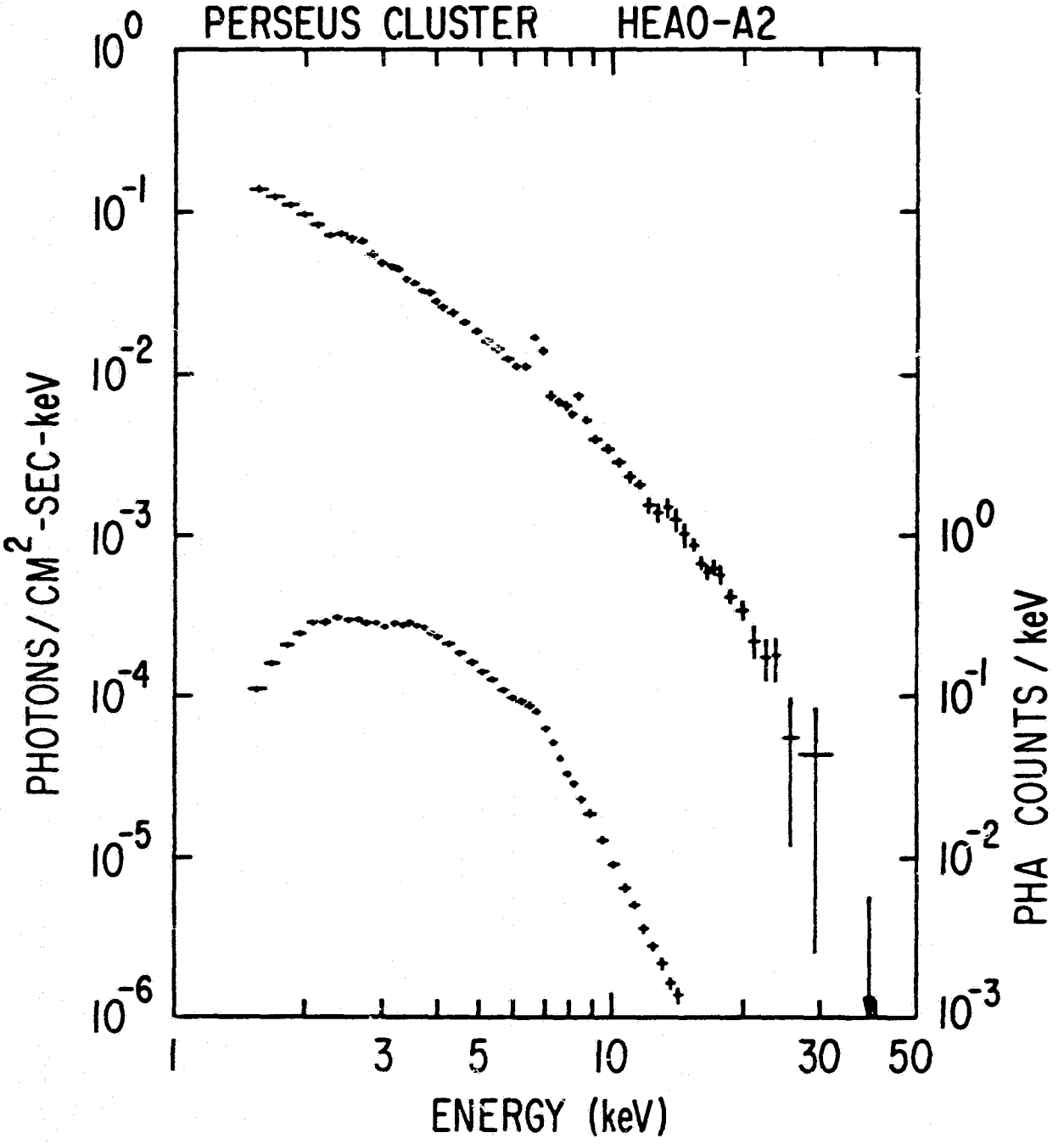
PERSEUS CLUSTER HEAO-A2
PHOTONS/CM^2-SEC-keV
PHA COUNTS / keV
ENERGY (keV)
10^0
10^{-1}
10^{-2}
10^{-3}
10^{-4}
10^{-5}
10^{-6}
1
3
5
10
30
50

Figure 1

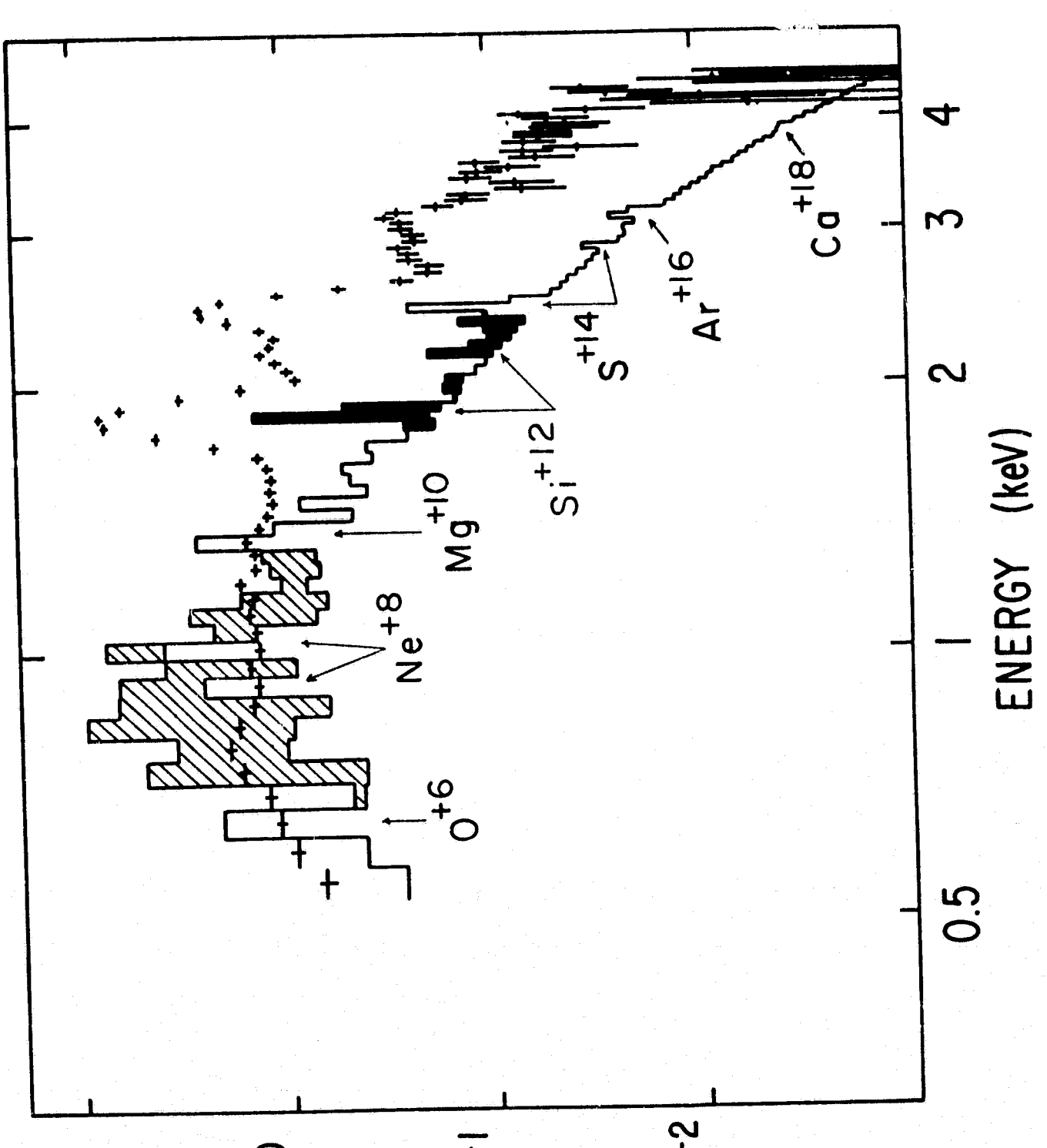

Figure 2

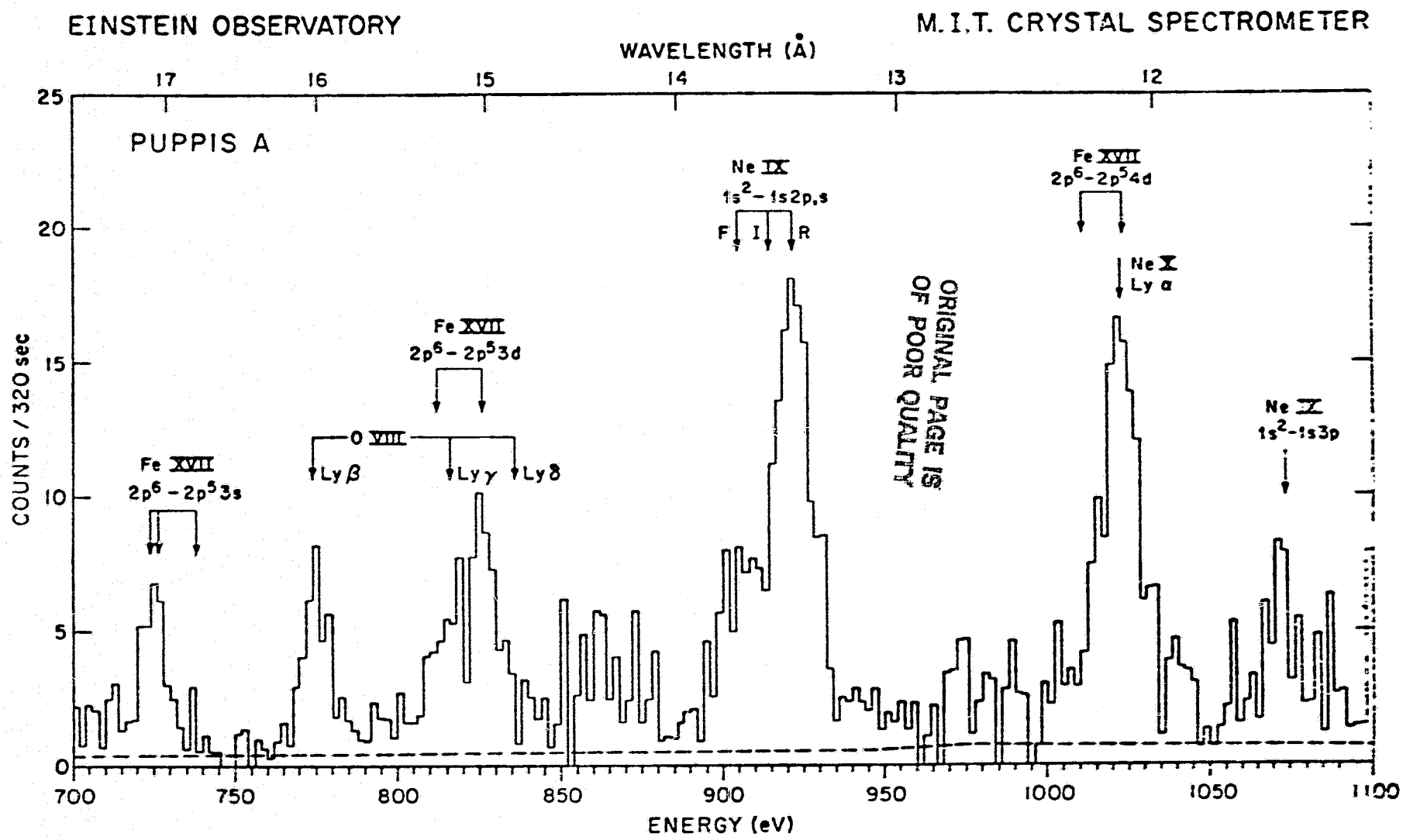
EINSTEIN OBSERVATORY
M.I.T. CRYSTAL SPECTROMETER
WAVELENGTH (Å)
17
16
15
14
13
12
PUPPIS A
Ne IX
1s²-1s2p,s
F
I
R
Fe XVII
2p⁶-2p⁵4d
Ne X
Ly α
Fe XVII
2p⁶-2p⁵3d
O VIII
Lyβ
Lyγ
Lyδ
Fe XVII
2p⁶-2p⁵3s
Ne IX
1s²-1s3p
ORIGINAL PAGE IS
OF POOR QUALITY
COUNTS / 320 sec
0
5
10
15
20
25
700
750
800
850
900
950
1000
1050
1100
ENERGY (eV)

Figure 3

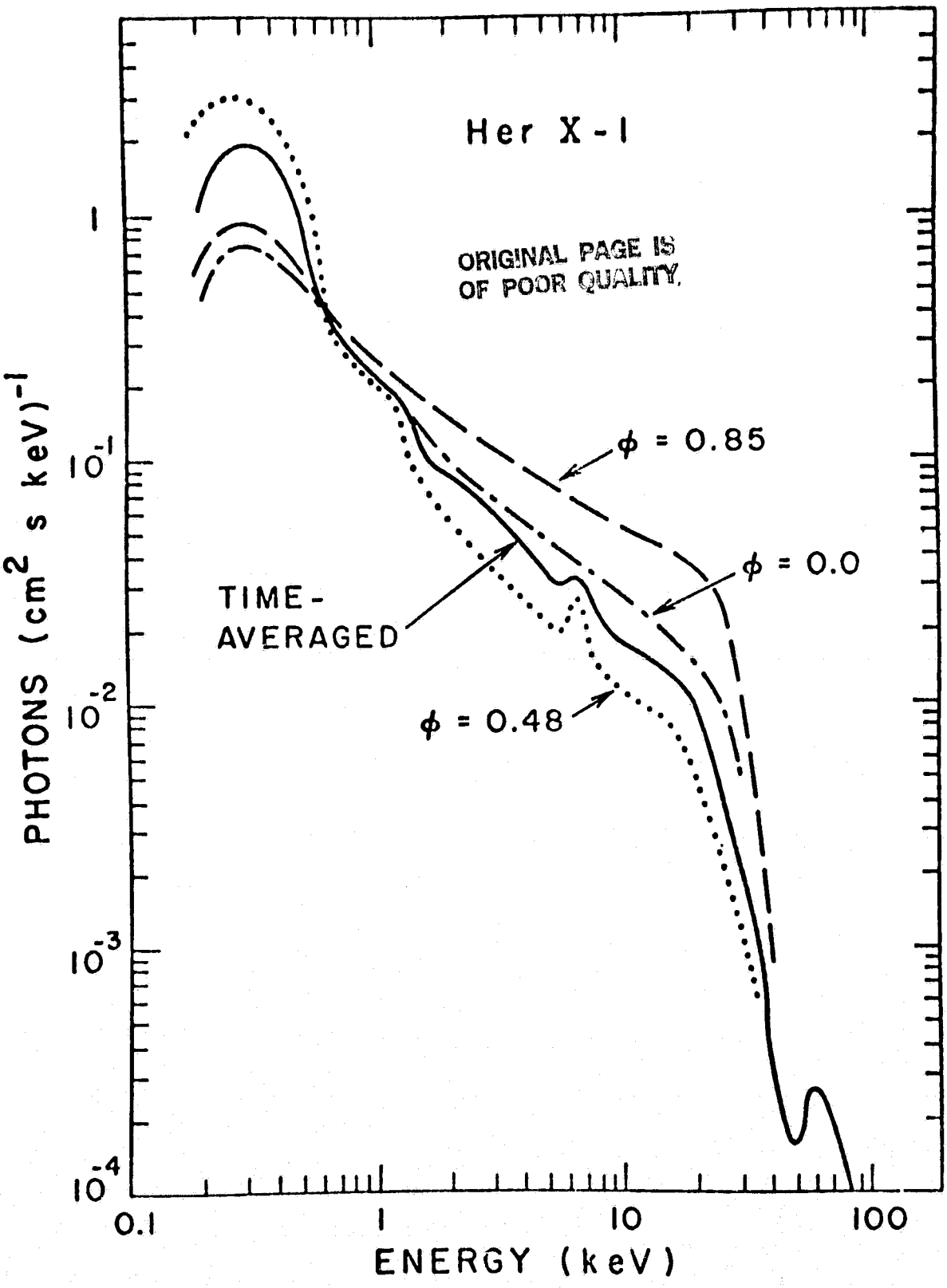
Her X-1
ORIGINAL PAGE IS
OF POOR QUALITY
PHOTONS (cm² s keV)⁻¹
1
10⁻¹
10⁻²
10⁻³
10⁻⁴
0.1
1
10
100
ENERGY (keV)
φ = 0.85
φ = 0.0
φ = 0.48
TIME-
AVERAGED

Figure 4